Aerosol and Air Quality Research

ORIGINAL RESEARCH
https://doi.org/10.4209/aaqr.210047

Particle-bound PAHs and Chemical Composition, Sources and Health Risk of $PM_{2.5}$ in a Highly Industrialized Area

Elizabeth Vega[1*‡], Diego López-Veneroni[2], Omar Ramírez[3], Judith C. Chow[4], John G. Watson[4]

[1] Instituto Mexicano del Petróleo, 07730 México, DF, México
[2] Independent Researcher, México
[3] Faculty of Engineering, Environmental Engineering, Universidad Militar Nueva Granada, Cajicá-Zipaquirá 250247, Colombia
[4] Division of Atmospheric Sciences, Desert Research Institute, Reno, NV 89512, USA

ABSTRACT

$PM_{2.5}$ monitoring campaigns were conducted in 2006, 2010, and 2011 in Tula, Hidalgo, Mexico, a highly industrialized area which includes a refinery, a thermoelectric power plant, five cement plants, limestone mining, and industrial waste combustion. These data establish baselines and trends against which later concentrations can be compared as emission reduction plans are implemented. $PM_{2.5}$ mass, chemical composition, and 15 particle-bound polycyclic aromatic hydrocarbons (PAHs) were measured at two sites. $PM_{2.5}$ masses ranged from 26 to 31 μg m^{-3}. Carbonaceous aerosols were the largest $PM_{2.5}$ component, accounting for 47–57% of the mass. Approximately 40–51% of the carbonaceous aerosol was attributed to secondary organic carbon. Ionic species accounted for 40–44% of $PM_{2.5}$, with sulfate being the dominant ion. The sum of particle-bound PAH concentrations ranged from 14–31 ng m^{-3}. Six factors derived from Principal Component Analysis (PCA) explained ~85% of the $PM_{2.5}$ variance. The derived factors were associated with sources based on marker species resulting in heavy-oil combustion (22% of variance), vehicle engine exhaust (13–19% of variance), fugitive dust (18% of variance), biomass burning (9–13% of variance), secondary aerosols (14% of variance), and industrial emissions (6–10% of variance). Combustion of solid waste (e.g., tires and industrial waste) of the recycling cement kilns and incinerators resulted in elevated toxic species such as, Cd, and Sb in the range of 0.02–0.3 μg m^{-3}. A health risk assessment of carcinogenic trace elements was performed showing that the total cancer risk decreased for both children and adults in 2010/2011 (ranging from 3.5×10^{-6} to 6.0×10^{-5}) as compared to 2006 (ranging from 8.6×10^{-7} to 5.7×10^{-6}). The inhalation life-time cancer risk (ILCR) for particle-bound PAHs ranged from 8.6×10^{-5} to 1.2×10^{-4}. Air quality can be improved by switching to cleaner fuels and benefit from the use of natural gas instead of fuel oil in the power plant.

Keywords: Industrial pollution, Chemical mass closure, Fine particles, Polycyclic aromatic hydrocarbons, Risk assessment

OPEN ACCESS

Received: March 3, 2021
Revised: July 2, 2021
Accepted: July 28, 2021

* **Corresponding Author:** evega@atmosfera.unam.mx

‡ **Present address:** Centro de Ciencias de la Atmósfera, UNAM, 04510 Ciudad de México, CDMX, México

Publisher:
Taiwan Association for Aerosol Research
ISSN: 1680-8584 print
ISSN: 2071-1409 online

1 INTRODUCTION

Industrial activities are important contributors to poor air quality, particularly in developing countries (Silva *et al.*, 2021; Taiwo *et al.*, 2014) and when many of them are clustered together. Past studies find that air pollution increases the risk of respiratory and cardiovascular diseases (Du *et al.*, 2016), decreases the quality of life (Lee *et al.*, 2014), alters productivity (Zivin and Neidell, 2012), escalates medical costs (van Essen *et al.*, 2018), and generates adverse birth outcomes (Ha *et al.*, 2014). Industrial emissions of gases, particulate matter (PM), and toxic compounds are

being reduced by pollution control measures (Kwiatkowski *et al.*, 2021), and it is important to establish baselines against which to determine effectiveness of controls over time.

One of the largest industrial areas in Central Mexico is the Tula Industrial Corridor (TIC) located in the state of Hidalgo. This area comprises intensive industrial activities, including the Miguel Hidalgo refinery of Petróleos Mexicanos (PEMEX) and the Francisco Pérez Ríos thermoelectric power plant, the second and fifth largest complexes in the country, respectively. Other emitters include five cement plants, recycled alternative fuels combustion, industrial wastes, and limestone mining.

Emissions from Hidalgo State contribute to 21.7 MT y^{-1} of CO_2; 284,252 tons y^{-1} of CO; 115,162 tons y^{-1} of SO_2 (from which ~99% [113,868 tons y^{-1}] are from industries); 70,641 tons y^{-1} of VOC; 67,296 tons y^{-1} of NO_x; 21,997 tons y^{-1} of NH_3; 20,563 tons y^{-1} of PM_{10}; 15,176 of tons y^{-1} of $PM_{2.5}$; and 1,493 tons y^{-1} of black carbon (BC) (IEEH, 2011). In the study area, SO_2 emissions account for 10% of nationwide emissions, with 6% each for PM_{10}, $PM_{2.5}$ and NO_x (INECC, 2017). Under prevailing northerly winds, refinery and thermoelectric power plant emissions from the TIC have been detected in the northern sector of Mexico City (~60 km south) (García-Escalante *et al.*, 2014; Sosa *et al.*, 2013; Zambrano *et al.*, 2009).

Since the TIC was identified as one of the most polluted zones in Mexico, limited studies of gaseous, $PM_{2.5}$, and PM_{10} concentrations, emissions characterization, and air quality modeling were conducted (Almanza *et al.*, 2012; Camacho-López *et al.*, 2019; García-Escalante *et al.*, 2014; Martínez-Carrillo *et al.*, 2010; Montelongo-Reyes *et al.*, 2015; Querol *et al.*, 2008; Sosa *et al.*, 2013). Over the past decade, several studies on Mexico's PM chemical compositions have been carried out in urban (Ahmad *et al.*, 2021; Chen *et al.*, 2021; Manchanda *et al.*, 2021) and industrial areas (Duan *et al.*, 2021; Fadel *et al.*, 2021) such as Salamanca (Herrera *et al.*, 2012), Monterrey (Gonzalez *et al.*, 2016), Guadalajara (Murillo-Tovar *et al.*, 2018), Merida (Alvarez-Ospina *et al.*, 2021) and Mexico City (Amador-Muñoz *et al.*, 2011, 2020; Ladino *et al.*, 2018; Vega *et al.*, 2011).

This study complements these prior efforts by examining $PM_{2.5}$ chemical composition, including particle-bound polycyclic aromatic hydrocarbons (PAHs), during the years of 2006, 2010, and 2011. $PM_{2.5}$ organic and elemental carbon, ions, and PAH concentrations are used to identify major pollution sources. Toxic species associated with carcinogenic contaminants are used to evaluate health risks. The historical data set provides a baseline to assist policy makers in establishing control strategies and assessing the effectiveness of emission control measures over the past decade.

2 MATERIAL AND METHODS

2.1. Monitoring Sites

$PM_{2.5}$ and surface meteorology (i.e., wind speed [WS], wind direction [WD], atmospheric pressure [P], temperature [T], relative humidity [RH], and solar radiation [SR]) were measured at the Jasso (JAS) and Tepeji (TEP) sites (Fig. 1). The JAS site (99.31°W, 20.02°N) is located 5 km southwest of the Francisco Pérez Ríos power plant and the Miguel Hidalgo oil refinery. The site is adjacent to an open-pit limestone quarry, is surrounded by unpaved roads, and is influenced by traffic on major roads from the south and west. The TEP site (99.29°W, 19.86°N) is located 25 km south of the refinery, close to a highway and a major limestone mining area where cement materials are extracted. These sites were selected to assess emissions from major pollution sources and to determine their potential local and regional impacts.

2.2. Sampling and Analytical Methods

The first field campaign took place from 22 March to 22 April 2006 as part of the Megacity Initiative Local and Global Research Observations (MILAGRO). For comparison, additional 24-h $PM_{2.5}$ samples were also collected every third day at the same locations from 28 April to 28 of May 2010, and from 02 March to 30 April 2011.

Three different $PM_{2.5}$ samplers were used, including: 1) daily, 24-h (midnight to midnight) $PM_{2.5}$ samples by battery-powered portable MiniVol samplers (Airmetrics, Springfield, USA) at a flow rate of 5 L min^{-1}; 2) daily , 12-h daytime (06:00 to 18:00 h local time) and nighttime (18:00 h to next day 06:00 h) $PM_{2.5}$ samples by sequential filter samplers (SFS) at a flow rate of 113 L min^{-1} (Chow, 1995); and 3) daily denuder sampler (URG Corporation Carboro, NC, USA) at a flow rate of 16.7 L min^{-1}.

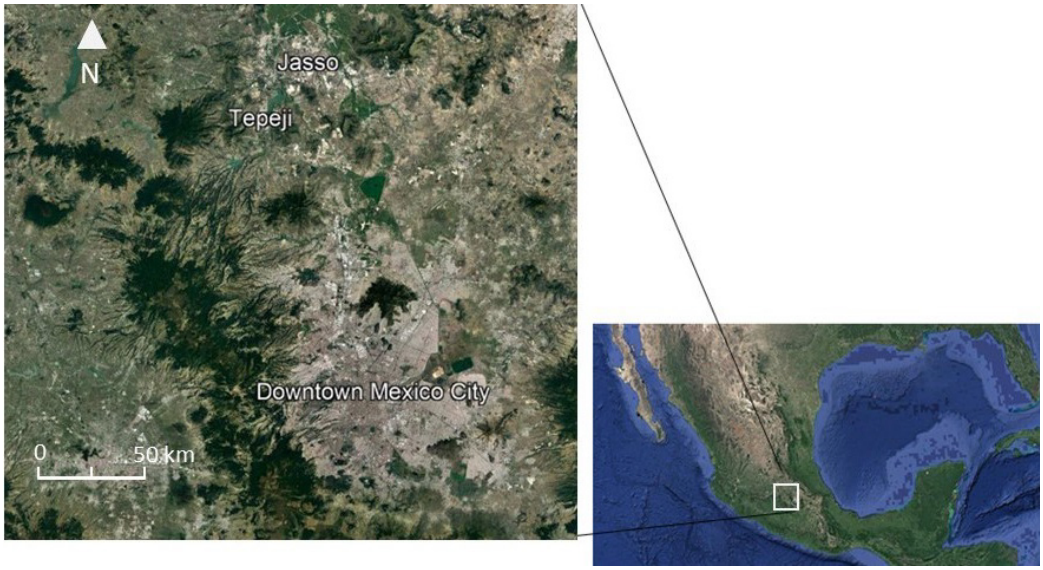

Fig. 1. Locations of Jasso (JAS) and Tepeji (TEP) monitoring sites in Hidalgo, Mexico.

MiniVol and SFS samples were collected on 47 mm diameter Teflon-membrane (Pall Gelman Laboratory) and quartz-fiber filters (Pallflex Gelman Sciences CT). Denuder samples used microfiber quartz-fiber filters (Whatman®, type QMA of 47 mm diameter). Teflon-membrane filters were equilibrated for 48-h in a controlled environment (35 ± 5% relative humidity and 20 ± 2°C temperature). Gravimetric analysis was conducted before and after sampling using a microbalance with ± 0.001 mg precision (AX 26 Mettler Toledo, Greifensee, Switzerland). After acid extraction, Teflon-membrane filters were analyzed for 20 elements (Li, Na, Mg, Al, Si, K, Ca, V, Cr, Fe, Ni, Zn, As, Y, Cd, In, Sn, Ba, Hg, and Pb) by Inductively Coupled Plasma-Mass Spectrometry (ICP/MS) (Agilent 7500a, Santa Clara, CA) (Vega *et al.*, 2011). Quartz-fiber filters were analyzed for eight water-soluble cations and anions (Na^+, NH_4^+, K^+ Mg^{2+}, Ca^{2+}, Cl^-, NO_3^-, and $SO_4^=$) by ion chromatography (IC Waters®, Alliance™, Milford, Massachusetts, USA); and for organic carbon (OC) and elemental carbon (EC) by DRI Model 2001 (Atmoslytic Inc., Calabasas, CA, USA) thermal/optical carbon analyzer following the IMPROVE thermal/optical reflectance (TOR) protocol (Chow *et al.*, 1993, 2001, 2007; Vega *et al.*, 2011).

U.S. EPA guidelines (http://sor.epa.gov) quantify the 16 PAHs as priority pollutants that are considered to be possible or probable human carcinogens. However, only 15 PAHs were reported due to the high uncertainties associated with the quantification of benzo[b]fluoranthene. For PAH analysis, microfiber quartz-fiber filters were ultrasonically extracted three times for 20 minutes each. The extract was concentrated to 1 mL in an ultra-pure nitrogen stream. Acetonitrile was added, filtered, and concentrated to 0.5 mL. A total of 120 samples were analyzed for 15 PAHs using Gas Chromatograph/Mass Spectrometry (Model 6890N GC/MS and 5973N Agilent Technologies, San José Calif. USA). Identification was confirmed by deuterated PAHs (Cambridge Isotope Laboratories, CIL) and quantification was performed using authentic standards (ChemService), with the addition of an internal standard of fluoranthene d-12. Data validation included examination of linearity with standards ($r > 0.99$) with a relative standard deviation (RSD) $< 3\%$. Recovery efficiencies were between 89% and 106% by using internal standards of deuterated PAHs.

2.3. Quality Assurance/Quality Control (QA/QC)

The analytical limits of detection (LODs) ranged from 0.45 ng m^{-3} (Li) to 128.40 ng m^{-3} (Hg) for ICP/MS; 6.30 ng m^{-3} (Na^+) to 24.53 ng m^{-3} (Ca^{2+}) for IC; 0.109 μg C m^{-3} for carbon analysis, and 19.6 ng m^{-3} (BkF) to 107.93 ng m^{-3} (NAP) for GC/MS. Twenty field blanks were collected and analyzed, representing 14% of the total samples. Average blank values for all species were below LODs. Analytical results were corrected by subtracting the average blank. Replicates were performed for at least 10% of the samples with results of less than 5% differences. Calibration curves were acceptable when correlation coefficients were greater than 0.99. QC standards were

analyzed before each sample run, after each group of 10 analyses, and at the end of each set of analysis. Precision was verified by analyzing a sample 10 times with a mixture of species. Data were submitted to three levels of data validation, as documented in Chow *et al.* (2002).

2.4. Mass Closure and Secondary Organic Carbon (SOC)

$PM_{2.5}$ reconstruction requires indirect estimates of unmeasured species to achieve closure between measured gravimetric mass and sum of components as shown in Eq. (1) (Chow *et al.*, 2015):

$$PM = \text{Inorganic ions} + 1.4 \times OC + EC + \text{geological minerals} + \text{salts} + \text{non-geological elements} + \text{others} \quad (1)$$

To examine the extent of inorganic ion neutralization, ammonium (NH_4^+) concentrations were estimated based on the stoichiometric ratios of ammonium salts and compared to the IC measurements. It is assumed that particulate nitrate is present as ammonium nitrate (NH_4NO_3) and sulfate is present in the form of ammonium sulfate ($(NH_4)_2SO_4$), or ammonium bisulfate (NH_4HSO_4). Therefore, calculated ammonium equals 0.192 × sulfate + 0.29 × nitrate (Chow *et al.*, 2015). The ion balance showed that there was not enough NH_4^+ to fully neutralize SO_4^{2-}, suggesting the presence of NH_4HSO_4 and sulfuric acid (H_2SO_4). This is typical of local, rather than regional, SO_4^{2-}, as a longer residence time usually allows the non-neutralized SO_4^{2-} to come into contact with ammonia (NH_3).

OC may be of primary origin from combustion processes (e.g., wildfires, fireplaces, waste burning, and vehicles emissions) and secondary when formed in the atmosphere by photochemical reactions involving VOCs (Castro *et al.*, 1999). EC is a primary emission from incomplete combustion of fossil fuels or biomass burning and the OC/EC ratio is often used to separate primary from secondary organic carbon (SOC) according to Eq. (2) (Turpin and Huntzicker, 1995; Ramírez *et al.*, 2018):

$$SOC = OM - EC \times (OC/EC)_{min} \quad (2)$$

where organic mass (OM) is 1.4 × OC to account for unmeasured oxygen and hydrogen associated with carbon); and $(OC/EC)_{min}$ is the minimum ratio observed, representing primary aerosol. A $(OC/EC)_{min}$ ratio of 1.2 was used as it was the average of the minimum ratios observed. This value agrees with the $(OC/EC)_{min}$ = 1.1 measured for diesel engine exhaust (Viidanoja *et al.*, 2002).

2.5. Source Identification

Principal Component Analysis (PCA) was applied to identify associations among the measured components and possible $PM_{2.5}$ sources for samples collected in 2006 and 2011. A correlation matrix (IBM SPSS STATISTICS software V. 26) of the ambient concentrations was examined (Ahmad *et al.*, 2020; ChooChuay *et al.*, 2020). The Varimax rotation was used to maximize (or minimize) loading factors of each species, leading to large eigenvector values (loading) toward one and small loadings toward zero. Species with communality > 0.70 and values > 0.32 (Han *et al.*, 2006) were considered for association of factors with sources.

2.6. Health Risk Estimates

Risk analysis uses human equivalent concentrations to develop inhalation unit risks (IUR) and inhalation cancer slope factors (U.S. EPA, 2009). This approach is based on a linear extrapolation from exposures observed in animal and human occupational studies and is conservatively protective of public health (U.S. EPA, 2005). IUR is defined as the upper-bound excess lifetime cancer risk estimated from continuous exposure to an agent at a concentration of 1 μg m^{-3} in air (U.S. EPA, 2008). This approach has been used in recent studies on health risks of $PM_{2.5}$ (Nirmalkar *et al.*, 2021; Xu *et al.*, 2021).

The health risk associated with carcinogenic contaminants was estimated based on the assumption that inhalation is the major exposure pathway to trace elements following the criteria established by the U.S. EPA (2011). The selected toxic elements include As, Cd, Co, Cr (VI), Ni, and Pb, which are considered possibly/probably carcinogenic to humans by the International

Agency for Research on Cancer (IARC) (1990, 2006a, b, 2012). It assumed that the proportion of carcinogenic Cr (VI) to non-carcinogenic Cr (III) concentrations in ambient air is 1:6 (Hsu *et al.*, 2016), and the concentration of the Cr (VI) was 1/7 of the total Cr concentration (Park *et al.*, 2008; Ramírez *et al.*, 2020). Adults and children living in the study area were considered potential receptors. The Individual Cancer Risk (ICR) calculation is shown in Eq. (3):

$$ICR_{inhalation} = ExCo \times IUR \quad (3)$$

where $ICR_{inhalation}$ (dimensionless) represents individual lifetime cancer risk through inhalation of carcinogenic elements; ExCo is exposure concentration (μg m^{-3}); and IUR is the Inhalation Unit Risk (μg $m^{-3})^{-1}$ provided by the Integrated Risk Information System (IRIS) (https://www.epa.gov/iris), the Office of Environmental Health Hazard Assessment (OEHHA) (https://oehha.ca.gov), and the National Research Council (2000). Generally, acceptable or tolerable $ICR_{inhalation}$ for regulatory purposes range between 1×10^{-6} and 1×10^{-4} (U.S. EPA, 2011). ExCo were calculated with Eq. (4):

$$ExCo = Ct \times ET \times EF \times ED/AET \quad (4)$$

where Ct is the carcinogenic element concentration in $PM_{2.5}$ (μg m^{-3}); ET is the exposure time set at 24 hours day^{-1}; EF is the exposure frequency set at 365 days $year^{-1}$; ED is the exposure duration set at 6 and 24 years for children and adults, respectively (Wang *et al.*, 2018); and AET is the average exposure time (hours = 75 years × 365 days $year^{-1}$ × 24 h day^{-1}), where 75 years is the life expectancy in Mexico (Gobierno de Mexico, 2019).

The health risk associated with exposure to PAHs was estimated by calculating the benzo(a)pyrene (BaP) equivalent concentration (BaP_{eq}) with Eq. (5) and the inhalation life-time cancer risk (ILCR) with Eq. (6):

$$BaP_{eq} = \sum_{i=1}^{n} C_i \times TEF_i \quad (5)$$

$$ILCR = BaP_{eq} \times UR_{BaP} \quad (6)$$

where C_i and TEF_i are the mass concentration and the toxic equivalency factor of individual PAHs, respectively. The TEF for naphthalene (NAP), acenaphthene (ACE), acenaphthylene (ACY), flouranthene (FLA), phenanthrene (PHE), fluorene (FLU), and pyrene (PYR) is 0.001; for anthracene (ANT), chrysene (CHR) and benzo[ghi]perylene (Bg)P is 0.01; for benzo[a]anthracene (BaA), benzo[k]flouranthene (BkF), and indeno[1,2,3-cd]pyrene (IND) is 0.1; and for benzo[a]pyrene (BaP) and dibenzo[a,h]anthracene (DbA) is 1 (Nisbet and LaGoy, 1992; Shen *et al.*, 2019). UR_{BaP} is the inhalation cancer unit risk of BaP (8.7×10^{-5} ng m^{-3}) for a lifetime of 70 years exposure to 1 ng m^{-3} of BaP (WHO, 2000; Mehmood *et al.*, 2020).

3 RESULTS

3.1. Meteorological Aspects

Meteorological conditions during the MILAGRO campaign have been reported by Sosa *et al.* (2013). Surface meteorological variables of T, RH, WP, and P showed similar patterns at the two sites with maximum T (24°C) reached in the afternoon (16:00–17:00 h, local time) and minimum T (8.5–12°C) during morning (07:00–08:00 h) (Supplemental Fig. S1). The large thermal oscillation of ~16°C is typical of the area. Solar radiation was at its maximum at 14:00–15:00 h, just before the maximum temperature occurred. Solar radiation at TEP was twice that at JAS. Maximum RH occurred at night with the minimum at 16:00–17:00 h. The minimum WS was found at night and early morning, with maxima during 19:00–20:00 h, and WS was two times higher at JAS as compared to TEP.

Meteorological conditions showed similar patterns at the two sites in 2010 and 2011 (Fig. S2) with maximum T (32°C) reached in the afternoon (14:00–16:00 h, local time) and minimum T (2.6–3.2°C) during morning (06:00–07:00 h). Solar radiation was at its maximum at 12:00–13:00 h.

Maximum RH occurred at night with the minimum at 15:00–17:00 h. The minimum WS was found at night and early morning, with maximum during 15:00–18:00 h. Average WS was twofold higher in TEP as compared to JAS.

Table S1 shows a decreasing trend of $PM_{2.5}$ concentrations from 2006 to 2011, with a three-year average of 26.8 and 24.0 μg m^{-3} at the JAS and TEP sites, respectively. Average 24-hr $PM_{2.5}$ concentrations at JAS (31 μg m^{-3}) and TEP (26 μg m^{-3}) for 2006 were below the Mexican National Ambient Air Quality Standard (NAAQS) of 65 μg m^{-3}. Concentrations in JAS were reduced by 10% (2010) and 30% (2011) at JAS and 1% (2010) and 19% (2011) at TEP. During 2006, $PM_{2.5}$ concentrations were associated with temperature and inversely correlated with wind speed (Sosa *et al.*, 2013). Low WS (< 2 m s^{-1}) from ENE and ESE winds at the TEP and moderate WS (2.6 m s^{-1}) from the SW at the JAS were associated with the highest $PM_{2.5}$concentrations.

Murillo-Tovar *et al.* (2018) found that lower photochemical activities during cold-dry season inhibit atmospheric chemical reactions and enhance ambient PAHs concentrations, partially due to the stronger tendency of PAH to bond particles. Reduction of PAHs has been found during the rainy season due to wet deposition. In addition, it may alter the irradiance and ozone concentrations that effect photo-oxidation during the cold-dry season (Amador *et al.*, 2020).

3.2. Chemical Composition and Material Balance

Mass and chemical composition of ~200 $PM_{2.5}$ samples from the 2006 campaign were used to identify emission sources. High correlations (r = 0.9) were found between water soluble ions and the sum of measured species. $PM_{2.5}$ calcium (Ca) includes both water-soluble and -insoluble oxides resulting in a low anion versus cation correlation (r = 0.62). The correlation improved considerably (r = 0.94) when Ca^{2+} was removed. Tables S2 and S3 show average and maximum 12-h and 24-h $PM_{2.5}$ mass and chemical composition of $PM_{2.5}$ concentrations in JAS and TEP, respectively. Yearly (2006, 2010, and 2011) comparisons are summarized in Tables 1 and 2.

Larger decreases were found for most species from 2006 to 2010/2011. Average and maximum SO_4^{2-} concentrations were reduced by > 50% at JAS and by ~20% at TEP from 2006 to 2011. Total carbon (sum of OC and EC) was reduced by 45–55% from 2006 to 2011. Compared to 2006, more

Table 1. Average and maximum 24-h chemical $PM_{2.5}$ compositions (μg m^{-3}, [a] ng m^{-3}) at Jasso, Hidalgo.

	2006		2010		2011	
	Average ± SD	Max	Average ± SD	Max	Average ± SD	Max
Mass	31.03 ±0 .93	52.04	27.94 ± 0.87	38.55	21.54 ± 0.49	30.25
Nitrate (NO_3^-)	1.03 ± 0.10	2.11	2.48 ± 0.24	4.44	0.40 ± 0.02	0.70
Sulfate (SO_4^{2-})	7.52 ± 0.59	12.04	8.05 ± 0.65	12.34	3.42 ± 0.16	5.86
Ammonium (NH_4^+)	2.81 ± 0.19	4.35	2.95 ± 0.24	7.37	1.26 ± 0.06	2.17
Soluble potassium (K^+)	0.23 ± 0.02	0.43	0.39 ± 0.04	0.77	0.13 ± 0.01	0.19
Soluble magnesium (Mg^{2+})	0.07 ± 0.02	0.11	0.08 ± 0.01	0.12	0.01 ± 0.00	0.02
Soluble calcium (Ca^{2+})	2.07 ± 0.15	6.22	0.92 ± 0.10	2.37	0.06 ± 0.00	0.15
Organic Carbon (OC)	7.96 ± 1.12	14.72	2.76 ± 0.31	4.49	4.71 ± 0.32	11.41
Elemental Carbon (EC)	3.55 ± 0.50	7.51	2.42 ± 0.39	4.98	1.68 ± 0.22	3.41
Aluminum (Al) [a]	88.6 ± 5.9	295.7	< 0.0	0.0	170.1 ± 09.3	323.3
Silicon (Si) [a]	258.6 ± 27.2	663.1	477.4 ± 44.9	1348.4	295.3 ± 27.7	553.6
Cobalt (Co) [a]	0.4 ± 0.0	0.8	< 0.0	0.0	0.1 ± 0.0	0.4
Vanadium (V)[a]	28.3 ± 3.2	64.2	74.7 ± 8.1	150.0	13.4 ± 0.3	61.3
Chromium (Cr) [a]	29.0 ± 1.6 0	37.4	< 0.0	0.0	4.6 ± 0.2	6.3
Nickel (Ni) [a]	0.4 ± 0.0	0.8	10.1 ± 0.9	30.5	2.0 ± 0.1	10.8
Zinc (Zn) [a]	10.4 ± 0.6	16.0	24.7 ± 3.1	92.0	26.2 ± 1.2	43.1
Arsenic (As) [a]	11.9 ± 0.6	20.9	< 0.0	0.0	0.1 ± 0.1	0.4
Molybdenum (Mo) [a]	1.0 ± 0.1	1.8	< 0.0	0.0	0.2 ± 0.0	0.8
Cadmium (Cd) [a]	3.7 ± 0.2	5.6	< 0.0	0.0	0.3 ± 0.1	0.6
Tin (Sn) [a]	5.6 ± 0.4	11.5	< 0.0	0.0	0. 9 ± 0.0	5.0
Antimony (Sb) [a]	3.2 ± 0.2	6.8	< 0.0	0.0	2.1 ± 0.1	6.5
Lead (Pb) [a]	19.5 ± 1.0	59.8	2.8 ± 0.3	16.6	3.0 ± 0.1	8.7

Table 2. Average and maximum of 24-h $PM_{2.5}$ chemical compositions (μg m^{-3}, [a]ng m^{-3}) at Tepeji, Hidalgo.

	2006		2010		2011	
	Average ± SD	Max	Average ± SD	Max	Average ± SD	Max
Mass	25.73 ±0.26	53.10	25.46 ± 0.79	36.21	20.81 ± 0.52	28.46
Nitrate (NO_3^-)	0.84 ± 0.08	2.19	0.90 ± 0.14	1.64	0.86 ± 0.04	1.28
Sulfate (SO_4^{2-})	6.40 ± 0.45	10.89	7.06 ± 0.48	11.67	5.27 ± 0.253	8.95
Ammonium (NH_4^+)	2.52 ± 0.17	4.16	2.60 ± 0.42	4.49	1.42 ± 0.07	3.62
Soluble potassium (K^+)	0.18 ± 0.012	0.30	0.24± 0.03	0.40	0.18 ± 0.02	0.31
Soluble magnesium (Mg^{2+})	0.05 ± 0.02	0.14	0.05 ± 0.01	0.07	0.02 ± 0.00	0.08
Soluble calcium (Ca^{2+})	0.37 ± 0.04	1.77	0.27 ± 0.06	0.41	0.58 ± 0.03	1.16
Organic Carbon (OC)	8.04 ± 1.09	14.88	2.29 ± 0.24	8.24	6.82 ± 0.44	10.13
Elemental Carbon (EC)	3.39 ± 0.46	6.71	1.24 ± 0.24	3.16	1.86 ± 0.32	3.06
Aluminum (Al) [a]	46.0 ± 2.7	239.7	20.0 ± 23.6	39.4	125.7 ± 5.7	181.3
Silicon (Si) [a]	162.9 ± 14.7	864.8	478.4 ± 68.9	648.0	264.2 ± 25.9	429.5
Cobalt (Co) [a]	0.4 ± 0.0	1.4	< 0.0	0.0	0.1 ± 0.0	0.1
Vanadium (V) [a]	20.6 ± 7.0	55.9	77.4 ± 11.4	213.8	37.6 ± 1.1	99.8
Chromium (Cr) [a]	101.5 ± 10.7	292.6	6.5 ± 17.6	6.5	8.9 ± 0.2	11.5
Nickel (Ni) [a]	0.4 ± 0.0	1.4	10.0 ± 1.5	33.7	7.7 ± 0.2	16.8
Zinc (Zn) [a]	9.3 ± 0.6	23.5	23.7 ± 3.8	103.2	31.0 ± 1.0	97.0
Arsenic (As) [a]	12.5 ± 0.7	36.3	< 0.0	0.0	0.7 ± 0.1	2.0
Molybdenum (Mo) [a]	0.9 ± 0.1	2.6	< 0.0	0.0	0.6 ± 0.0	1.3
Cadmium (Cd) [a]	3.7 ± 0.2	10.5	< 0.0	0.0	0.2 ± 0.1	0.4
Tin (Sn) [a]	8.4 ± 0.6	26.7	< 0.0	0.0	1.0 ± 0.0	2.6
Antimony (Sb) [a]	3.6 ± 0.2	10.9	< 0.0	0.0	1.4 ± 0.0	3.2
Lead (Pb) [a]	199.0 ± 10.9	784.8	6.1 ± 1.0	27.7	6.4 ± 0.1	26.6

OC concentration reductions were found for 2010 (65% in JAS and 70% in TEP) as compared to 2011 (40% in JAS and 13% in TEP). Reductions in EC concentrations were similar at both sites with > 30% in 2010 and ~45% in 2011. This is probably due to the compulsory switching from fuel oil to natural gas during 2010 at the electric power plant (Sosa *et al.*, 2020).

3.2.1 Water-soluble ions

Ionic species were higher at JAS than at TEP, accounting for 44% of the $PM_{2.5}$ in 2006 (with ~24% of anions and ~20% of cations). This fraction was reduced to 27% of the $PM_{2.5}$ in 2011 (with ~19% of anions and 8% of cations). Year-to-year variations of ionic species were not found at the TEP site. SO_4^{2-} was the dominant ion, with a maximum of 14.9 μg m^{-3} at JAS during daytime on 09 April 2006 (accounting for 33% of the $PM_{2.5}$ mass) and 15.4 μg m^{-3} at TEP during daytime on 11 April 2006 (accounting for 44% of the $PM_{2.5}$ mass). The reduction of 2–5 μg m^{-3} of SO_4^{2-} from 2010 to 2011 reflect changes from fuel oil to natural gas combustion.

High correlations were found between SO_4^{2-} and NH_4^+ ($r > 0.97$). Similar correlations were observed between the daytime and nighttime samples at both sites. At JAS, average 24-h $(NH_4)_2SO_4$ (10.3 μg m^{-3}) accounted for 33.4% of $PM_{2.5}$; higher during nighttime (32%) than daytime (26%) in JAS. Similar observation was found in TEP, with $(NH_4)_2SO_4$ (8.8 μg m^{-3}) accounted for 34% of $PM_{2.5}$; higher during nighttime (38%) than daytime (30%).

Average 24-h SO_4^{2-} concentrations (6.4–7.5 μg m^{-3}) at TIC in 2006 were higher than those found in the highly industrialized areas of Salamanca (5.3 μg m^{-3}), and Cadereyta (4.3 μg m^{-3}) in Central and Northern Mexico (Vega *et al.*, 2007). This is consistent with the transport and transformation of SO_2 to SO_4^{2-} from north to south.

Low correlations (r = 0.34–0.36) were found between 12-h average NH_4^+ with NO_3^-, with higher correlations (r = 0.74) during nighttime. NO_3^- levels were low in the range of 0.8 to 1.8 μg m^{-3}, accounting for 3.4% of water-soluble ions. These levels are lower than the 3.6 and 3.2 μg m^{-3}, reported in Mexico City by Querol *et al.* (2008) and Vega *et al.* (2011), respectively. Average 24-h NH_4NO_3 (1.86 μg m^{-3}) accounted for 6% for $PM_{2.5}$. Similar to those found from SO_4^{2-}, NO_3^- concentrations showed an overall 2.5-fold reduction from 2006 to 2011.

Table 3. Average 24-h and 12-h $PM_{2.5}$ organic mass (OM = OC × 1.4), elemental carbon (EC), secondary organic carbon (SOC), and primary organic carbon (POC) concentrations (μg m^{-3}) in Jasso (JAS) and Tepeji (TEP).

	JAS					TEP				
Year	2006			2010	2011	2006			2010	2011
Sampling Time	6–18 h	18–6 h	24-h	24-h	24-h	6–18 h	18–6 h	24-h	24-h	24-h
Carbon species										
OM	13.5	5.8	11.1	3.9	6.6	11.9	10.0	11.3	3.2	9.5
EC	4.1	1.3	3.6	2.4	1.7	2.9	2.3	3.4	1.2	1.9
SOC	8.5	4.2	6.9	1.0	4.6	8.4	7.3	7.2	1.7	7.3
POC	5.0	1.6	4.3	2.9	2.0	3.5	2.7	4.1	1.5	2.2

3.2.2 Carbonaceous aerosols

In 2006, carbonaceous aerosols (1.4 × OC + EC) accounted for 47% and 57% of 24-h $PM_{2.5}$ mass at JAS and TEP, respectively. These values fluctuated between 2.5% (6.3 μg m^{-3}) in 2010 and 38.4% (8.3 μg m^{-3}) in 2011 at JAS, and between 17.5% (4.4 μg m^{-3}) in 2010 and 54.8% (11.4 μg m^{-3}) in 2011 at TEP. The fraction of carbonaceous aerosol in $PM_{2.5}$ is consistent with the 50% measured in the Mexico City Metropolitan Area (MCMA; Johnson *et al.* (2006); 52% at Salamanca (Vega *et al.*, 2007); and 55% during the MILAGRO campaign (Querol *et al.*, 2008), but it is ~20% higher than concentrations found at Cadereyta (33% of $PM_{2.5}$; Vega *et al.*, 2009).

At JAS, the carbonaceous fraction in $PM_{2.5}$ consisted of 25.6% OC and 11.4% EC, over twofold higher during the daytime (9.6 μg m^{-3}) than at nighttime (4.1 μg m^{-3}). Average 24-h OC and EC concentrations were 8.0 and 3.4 μg m^{-3}, similar to those at TEP, with OC/EC ratios of 2.7. The extent of secondary aerosol formation and industrial emissions may affect the OC:EC ratios.

Table 3 summarizes the $PM_{2.5}$ carbon concentrations. Average $PM_{2.5}$ SOC concentrations were 6.9 and 7.3 μg m^{-3} in 2006, accounting for 22.0 and 28.0% of $PM_{2.5}$ mass and 40–51% of carbonaceous aerosol at JAS and TEP, respectively. SOC concentrations were reduced to 1.0 and 1.7 μg m^{-3} in 2010 and 4.6 and 7.3 μg m^{-3} in 2011 at the JAS and TEP sites, respectively. Daytime/nighttime ratios were 3 for POC and 2 for SOC at both JAS and TEP. Reduction of POC from 2006 were significant, with ~53% (2011) at JAS and 63% (2010) at TEP.

3.2.3 Geological material, salts, and trace elements

In 2006, geological material accounted for ~18.5% of 12-h $PM_{2.5}$ (daytime and nighttime) at JAS, consistent with nearby quarrying activities. Higher daytime (8% of $PM_{2.5}$) than nighttime (3%) geological contributions were found at TEP. Contributions from geological material were reduced to ~10% in 2010 and ~8% in 2011 at both sites.

Average Ca in the form of calcium oxide (CaO), attributed to the nearby limestone mining and quarries, accounted for 62% of 24-h $PM_{2.5}$ geological material. The highest 12-h CaO concentrations (7.5 and 7.3 μg m^{-3}) were found for daytime on 11 April and nighttime on 7 April 2006 at the JAS, accounting for > 31% of the geological material. This was likely due to prevailing northerly to northeasterly winds (4–9 m s^{-1}) during daytime hours with direct influence from upwind cement processes. Salts contribution were low, ranging from 0.38 to 0.71% of $PM_{2.5}$. Trace elements contributions ranged from 0.3 to 0.5% of 24-h $PM_{2.5}$ mass at the JAS and 0.9–1.7% at the TEP (Table 4).

Since 1996, the cement industries were allowed to burn both recycled alternative fuels and industrial wastes (e.g., coke, coal, tires, and solid and liquid hazardous waste), leading to higher emissions of metals and organic compounds (Jacott *et al.*, 2003; Arfala *et al.*, 2018). The use of alternative fuels reached 5% of the total fuel consumption in 2006 (Semarnat, 2008, 2016). Co-processing of industrial hazardous waste (e.g., tires and infectious biological waste) were authorized to 30 plants in 2010 (Semarnat, 2010). These toxic emissions may create health risks to local populations and to the environment (Cangialosi *et al.*, 2008).

Under the regulation of the Ministry of the Environment and Natural Resources (DOF, 2004), NOM-040-SEMARNAT-2002, the maximum air emission levels are 700 ng m^{-3} for the following ten elements: Sb, As, Se, Ni, Mn, Cd, Hg, Pb, Cr and Zn from a cement plant. Tables S2 and S3 show that maximum 24-h $PM_{2.5}$ concentrations were 2,926 ng m^{-3} for Cr and 6,388 ng m^{-3} for Fe

Table 4. Average $PM_{2.5}$ material balance (%) at the Tula Industrial Corridor, Mexico for sampling period from 22 March to 22 April 2006.

Site (Sampling Time)	Ammonium	Nitrate	Sulfate	Geological minerals[a]	Organics[b]	EC	Salt	Trace Elements[c]	Material Balance ($\mu g\ m^{-3}$)	Measured PM mass ($\mu g\ m^{-3}$)
JAS										
$PM_{2.5}$ (6–18 h)	7.97	2.77	21.87	18.68	36.16	10.48	0.38	0.31	38.20	45.46
$PM_{2.5}$ (18–6 h)	12.44	4.62	33.65	18.41	24.29	5.28	0.71	0.43	22.63	31.02
$PM_{2.5}$ (24–h)	9.28	3.51	24.81	12.18	36.40	11.60	0.41	0.48	30.52	31.03
TEP										
$PM_{2.5}$ (6–18 h)	10.23	2.56	26.73	7.95	40.37	9.25	0.50	0.99	29.82	35.52
$PM_{2.5}$ (18–6 h)	12.74	4.23	32.49	3.42	34.05	9.85	0.52	0.88	21.20	24.86
$PM_{2.5}$ (24–h)	9.83	3.27	24.97	4.11	41.86	12.50	0.58	1.67	26.37	25.73

[a] Geological minerals include 2.2 × Al, 2.49 × Si, 1.63 × Ca, and 2.42 × Fe.
[b] Organics include OC × 1.4.
[c] Trace elements include 20 ICP/MS elements, excluding geological species, such as Al, Si, Ca, No, Fe, Cl, and K.

at the TEP site. Elements such as Zn and Pb are related to incineration and open waste burning (Lucarelli *et al.*, 2019), although Pb may also be originated from other sources such as leaded gasoline, gasoline spills, lead smelting, coal combustion, and paint materials (Das *et al.*, 2018). In 2006, maximum 24-h Zn concentrations were 16 and 24 ng m^{-3}, while maximum Pb concentrations were 60 and 785 ng m^{-3} at the JAS and TEP sites, respectively. Large reductions of toxic species were found from 2006 to 2011: from 1,015 to 9 ng m^{-3} for Cr; from 1,990 to 6 ng m^{-3} for Pb in TEP; and from 15 to 5 ng m^{-3} for Cr; and from 20 to 3 ng m^{-3} for Pb in JAS. However, average 24-h Zn concentrations increased from 17 ng m^{-3} in 2006 to 26 and 31 ng m^{-3} in 2011 at the JAS and TEP sites, respectively.

Concentrations of other toxic air pollutants such as Cd, As, and Sb were low. Cd is a known human carcinogen, it causes damage to the lungs, kidneys, and bones (Satarug *et al.*, 2010). Average 24-h Cd concentrations were 8 ng m^{-3} in 2006 and decreased to 0.3 and 0.2 ng m^{-3} at the JAS and TEP sites, respectively. Maximum 24-h Hg concentrations from hazardous waste incinerator and a petrochemical plant reached 17.5 ng m^{-3} at JAS and 33.9 ng m^{-3} at TEP. Brake wear contains Fe, Cu, Ba, and Sb (Hagino *et al.*, 2016). A Cu/Sb ratio of 3.8 in this study, is consistent with the ratio of 4.6 by Hagino *et al.* (2016) used to identify brake wear.

3.2.4 Comparison with nearby measurements

Figs. 2 and 3 compare the major $PM_{2.5}$ ionic and metal concentrations, respectively, from the three sampling campaigns with those reported for PM_{10} from the TIC (Querol *et al.*, 2008; Martínez-Carrillo *et al.*, 2010). Collected PM_{10} samples were simultaneously collected at the JAS and TEP sites during the 2006 campaign (Querol *et al.*, 2008). Samples from Tlaxcoapan (TLA, a small agricultural town located 7.5 km NE from the TIC) were collected during July-December 2007 (Martinez-Carrillo, 2009). In addition, PM_{10} samples were collected at the T2 site (in a ranch ~50 km east of TIC at an elevated height [200 m]) from the MILAGRO campaign (Querol *et al.*, 2008).

The upper panel of Fig. 2 shows that the $PM_{2.5}$ fraction was mostly composed of Si and SO_4^{2-}, ~one to three orders of magnitude higher than K and Ca. The relatively high concentrations of the crustal element K in $PM_{2.5}$ at both sites is consistent with fugitive dust contributions. In contrast, Ca is the major species in the PM_{10} fraction at TLA and JAS, consistent with the operation of limestone processing. The relatively high abundance of Ca in PM_{10} suggests that coarse particle (PM_{10} minus $PM_{2.5}$) Ca is mostly produced by limestone quarries and cement industry.

The metal components of both $PM_{2.5}$ and PM_{10} samples in Fig. 3 at JAS showed elevated V and Zn. At TEP, Pb and Cr were abundant in both the coarse and fine particle sizes, consistent with anthropogenically derived activities. PM_{10} ionic and metal concentrations from site T2 (Querol *et al.*, 2008) were low, reflecting less impact from the anthropogenic activities.

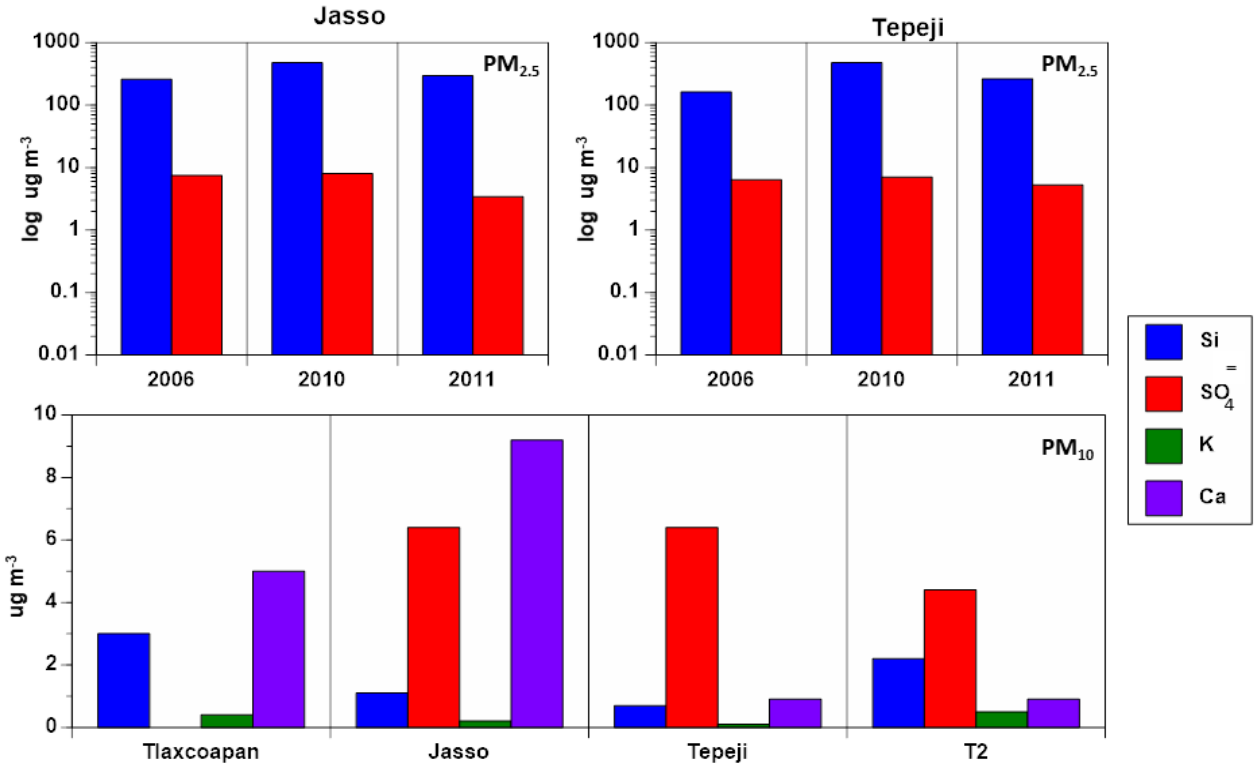

Fig. 2. Comparison between silicon (Si), sulfate (SO_4^{2-}), and elemental potassium (K) and calcium (Ca) from this study (upper panel), with PM_{10} species (lower panel) collected in and around the Tula Industrial Corridor (Martínez-Carrillo *et al.*, 2010; Querol *et al.*, 2008).

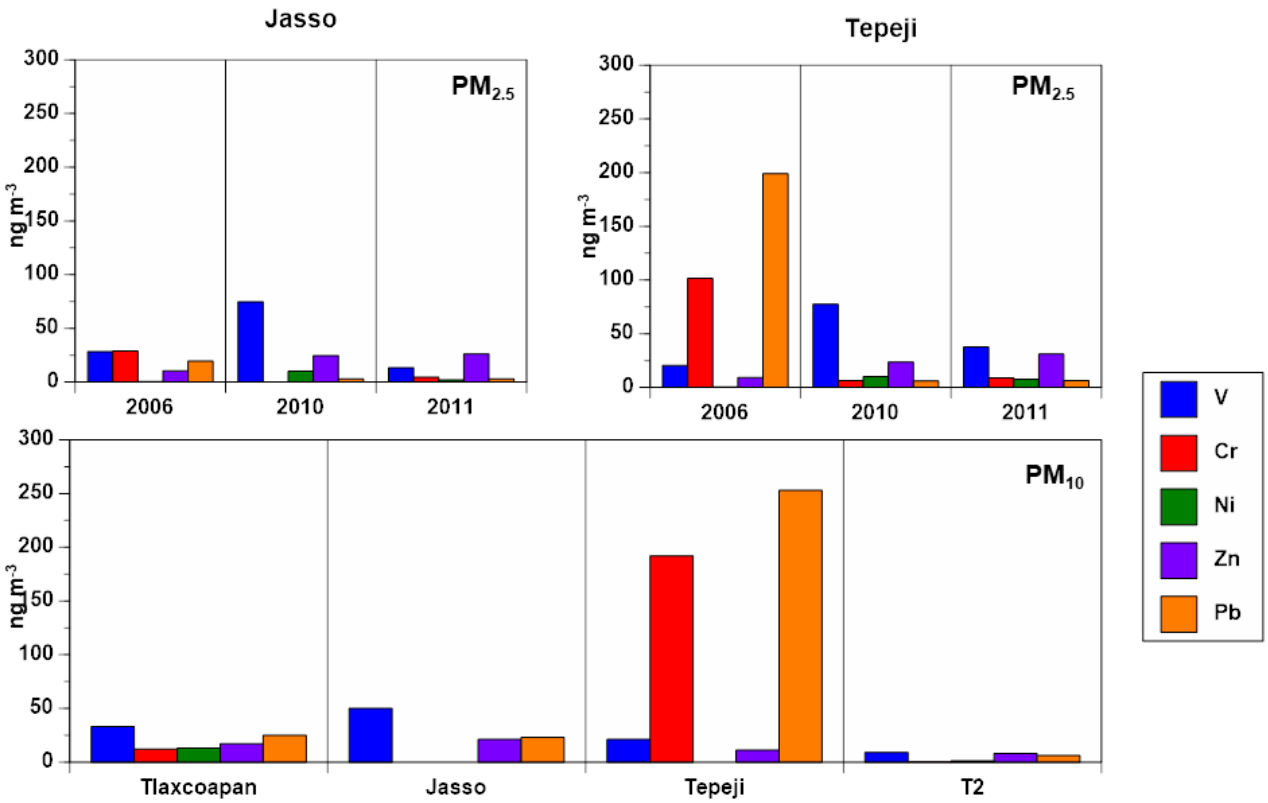

Fig. 3. Comparison between $PM_{2.5}$ metal concentrations from this study (upper panel), with PM_{10} metal concentrations (lower panel) collected in and around the Tula Industrial Corridor (Martínez-Carrillo *et al.*, 2010; Querol *et al.*, 2008).

Table 5. Statistical summary of average 24-hour $PM_{2.5}$ PAHs concentrations (ng m^{-3}) for 22 March to 22 April, 2006 at the Jasso (JAS) and Tepeji (TEP) sites, Hidalgo.

Element	JAS		TEP	
	Average ± SD	Maximum	Average ± SD	Maximum
Naphthalene (NAP)	1.91 ± 0.17	2.79	1.43 ± 0.19	1.96
Acenaphthene (ACE)	1.72 ± 0.19	2.95	1.43 ± 0.18	1.89
Acenaphthylene (ACY)	2.42 ± 0.26	4.00	2.03 ± 0.27	2.66
Fluorene (FLU)	2.26 ± 0.24	3.71	1.88 ± 0.25	2.48
Anthracene (ANT)	2.26 ± 0.25	3.81	1.85 ± 0.24	2.42
Phenanthrene (PHE)	1.49 ± 0.16	2.26	1.20 ± 0.15	1.80
Fluoranthene (FLA)	0.18 ± 0.09	0.86	0.22 ± 0.16	1.59
Benzo[a]anthracene (BaA)	0.48 ± 0.12	1.21	0.46 ± 0.19	1.99
Benzo[k]fluoranthene (BkF)	0.58 ± 0.22	2.07	0.32 ± 0.10	0.92
Chrysene (CHR)	0.24 ± 0.13	0.98	0.19 ± 0.14	1.25
Pyrene (PYR)	0.32 ± 0.08	0.89	0.36 ± 0.17	1.93
Benzo[a]pyrene (BaP)	0.56 ± 0.39	3.83	0.44 ± 0.28	2.84
Dibenzo[a,h]anthracene (DbA)	0.47 ± 0.12	1.17	0.29 ± 0.05	0.60
Benzo[ghi]perylene (BgP)	0.99 ± 0.23	2.34	0.85 ± 0.28	2.77
Indeno[1,2,3-cd]pyrene (IND)	1.62 ± 0.28	2.77	1.47 ± 0.42	4.42
∑15-PAH	17.5 ± 1.85	30.7	14.4 ± 1.52	22.8

3.3. Average $PM_{2.5}$ PAH Concentrations

The average of total PAHs (sum of 15 PAHs) at JAS (17.5 to 185 ng m^{-3}) was 18% higher than that at TEP. Table 5 shows that total PAHs were lower than 50 to 310 ng m^{-3} reported at traffic-intersections in Mexico City (Marr *et al.*, 2004). Elevated PAHs were found for acenaphthylene (ACY), fluorene (FLU), anthracene (ANT), naphthalene (NAP), and acenaphthene (ACE). Maximum benzo[a]pyrene (BaP), a marker for fossil fuels combustion, petroleum cracking, and vehicular emissions (Zhang *et al.*, 2019), was 3.8 and 2.8 ng m^{-3} at JAS and TEP, respectively. On-road studies in Mexico City showed good associations between benzo[ghi]perylene (BgP) from gasoline vehicles emissions and morning rush hours (Dzepina *et al.*, 2007). The results found in this study are lower than those reported in MILAGRO, with an average total PAHs concentration of 114.0 ng m^{-3} north of Mexico City (site T0, Instituto Mexicano del Petróleo), and 7.0 ng m^{-3} South of Mexico City (Pedregal) (Thornhill *et al.*, 2008). Table 6 compares PAH concentrations with those from urban or industrial areas in U.S.A., China, India, Spain, and Kenya. Except for the elevated concentrations at Nairobi, Kenya, PAHs from this study are one to several orders of magnitude higher than the industrial areas in other countries.

The average BaP/IND ratio of 0.35 in this study indicates photooxidation of BaP, due to higher irradiance in the warm dry season. Higher BaP/IND ratios were reported in Mexico City, with 0.67 during March 2006 and 2017 and 0.93 in November, attributing to lower BaP photo-oxidation (Amador *et al.*, 2020).

3.4. Principal Component Analysis

Table 7 summarizes the eight factors identified by PCA, explaining 91–92% of the total $PM_{2.5}$ variance, with the inclusion of PAHs in 2006. Cement production emissions were the major factor representing 29% of the total variance, on average. This factor is characterized by the presence of OC, EC, Co, and Ni as markers of heavy-oil combustion processes (Hsu *et al.*, 2016). Recycled alternative fuels, including tires and industrial wastes, explain the high factor loadings of Hg, Cd, Sb, Cr, Pb, Cu, and Zn (Hua *et al.*, 2016). The second factor (15–17% of variance) is associated with mixed industrial emissions marked by PAHs such as FLU, PHE, and ANT, representing emission from coking, steelworks, and use of gas (Wang *et al.*, 2020). The third factor (14% of variance) is characterized by markers of soil and fugitive dust such as Fe, Mg, Si, Ca and Al. The presence of Ca^{2+} indicates contributions from limestone quarries (Galindo *et al.*, 2011). The fourth factor is associated with vehicle engine exhaust emissions (11–17% of variance), characterized by PAHs such as FLA, BaA, PYR, CHR, and BkF, indicative of vehicle emissions (Wang *et al.*, 2020). The fifth

Table 6. Comparison of $PM_{2.5}$ PAH concentrations (ng m^{-3} and * pg m^{-3}) in the Tula Industrial Corridor, with other studies.

Element	Industrial (This study)	Urban California, USA*[a]	Urban Guangzhou, China[b]	Industrial Nunhai, India[c]	Industrial Tarragona, Spain[d]	Industrial Nairobi, Kenya[e]
Naphthalene (NAP)	1.67	6.48	0.4	-	0.24	-
Acenaphthene (ACE)	1.58	1.41	0.02	0.04	0.11	-
Acenaphthylene (ACY)	2.23	-	0.08	-	0.10	-
Fluorene (FLU)	2.07	6.19	0.10	0.02	0.56	1.80
Anthracene (ANT)	2.06	2.53	0.10	0.11	0.64	1.70
Phenanthrene (PHE)	1.35	30.05	1.10	0.04	0.26	7.80
Fluoranthene (FLA)	0.20	36.03	1.70	0.01	0.17	7.60
Benzo[a]anthracene (BaA)	0.47	28.75	0.80	0.06	0.30	5.00
Benzo[k]fluoranthene (BkF)	0.45	34.80	1.00	0.15	1.05	3.10
Chrysene (CHR)	0.22	43.65	1.60	0.03	0.39	7.80
Pyrene (PYR)	0.34	52.35	1.60	0.02	0.38	11.50
Benzo[a]pyrene (BaP)	0.50	65.08	1.60	0.14	0.39	5.00
Dibenzo[a,h]anthracene (DbA)	0.38	7.76	0.30	0.25	0.42	0.60
Benzo[ghi]perylene (BgP)	0.92	143.33	2.60	0.18	0.47	15.80
Indeno[1,2,3-cd]pyrene (IND)	1.55	70.08	2.50	0.09	0.32	-

[a] Eiguren *et al.*, 2004; [b] Yang *et al.*, 2010; [c] Rajput *et al.*, 2009;.[d] Ramirez *et al.*, 2011; [e] Muendo *et al.*, 2006.

factor (6–7% of variance) is characterized by secondary aerosols mixed with markers of oil combustion such as V and Ni at Jasso (Corbin *et al.*, 2018). The sixth factor (5–6% of the variance) is associated with biomass combustion with markers such as NO_3^-, BaP, BkF, Cl^-, Pb, and K^+ at Jasso (Manousakas *et al.*, 2017; Wang *et al.*, 2020), and OC, EC, and K^+ at TEP (Bernardoni *et al.*, 2011). The seventh factor (3–4% of variance) is characterized by crude oil with markers such as V and Ni (Manousakas *et al.*, 2017). The eighth factor (3–6% of variance) represents the metal manufacturing industry, associated with As and Cu at JAS, and Pb, Cl^-, and Sn at TEP (Hedberg *et al.*, 2005; Taiwo *et al.*, 2014).

When PAHs are deleted from the PCA analysis, Table 8 shows that five factors were identified, explaining 86-88% of the total $PM_{2.5}$ variance in 2006. Cement kiln emissions remain as the major factor, explaining 36% of the total variance, with markers of heavy-oil combustion (Co, Ni, OC and EC) and recycled alternative fuels (Hg, Cd, Sb, Cr, Pb, Cu, and Zn) (Hsu *et al.*, 2016). The second factor (21% of variance) is fugitive dust with markers such as Fe, Mg, Si, Ca^{2+}, and Al. The third factor (15% of variance) is heavy-oil combustion processes with markers such as SO_4^{2-}, V, and Ni (Manousakas *et al.*, 2017; Corbin *et al.*, 2018). The fourth factor (5–9% of variance) is characterized by Cl^- and Pb, associated to recycled alternative fuels and metal manufacturing industries at TEP (Galindo *et al.*, 2011; Taiwo *et al.*, 2014), and Cu related to metal - mechanic industries at JAS (Taiwo *et al.*, 2014). The fifth factor (8% of variance) is biomass combustion characterized by OC, EC, and K^+ at TEP (Bernardoni *et al.*, 2011), and NO_3^-, Cl^-, Pb, and K^+ at JAS (Manousakas *et al.*, 2017; Wang *et al.*, 2020).

Table 9 summarizes PCA identified factors, explaining 84–85% of the total $PM_{2.5}$ variance in 2011. Oil combustion is the major factor, representing on average 22% of the total variance. This factor is characterized by V and Ni (Manousakas *et al.*, 2017; Corbin *et al.*, 2018; Khan *et al.*, 2021), originating from the refinery and thermoelectric plants. The presence of Mo at JAS and TEP suggests emissions from catalysts in the petrochemical process (Minocha and Goyal, 2013). The presence of Ca^{2+} shows contributions of cement plants, particularly at TEP (Gupta *et al.*, 2012). The second factor (13–19% of variance), is associated with vehicle engine exhaust emissions, marked by the high contribution of OC and EC. Zn is used as an additive in lubricating oil (Liu *et al.*, 2017). The presence of Zn, Sb, Cd, and Cu are associated with non-exhaust emissions from road traffic (Taiwo *et al.*, 2014; Hsu *et al.*, 2016), and elements such as Fe, Al, Si, and Ca are related to road dust resuspension (Bernardoni *et al.*, 2011). The third factor (17–18% of variance) is characterized by markers of soil and fugitive dust such as Si, Mg, Al, and Fe (Martínez-Carrillo *et al.*, 2010; Khan *et al.*, 2021). The presence of Ca^{2+} indicates contributions from limestone

Table 7. Principal component analysis (PCA[a]) for $PM_{2.5}$ including PAHs at the Jasso (JAS) and Tepeji (TEP) sites during 2006.

	JAS									TEP							
	Cement kiln	Mixed industry	Dust	Traffic	Sec. aerosols	Biomass burning	Oil combustion	Metal industry		Cement kiln	Mixed industry	Dust	Traffic	Sec. aerosols	Biomass burning	Oil combustion	Metal industry
Ba	**0.97**								Co	**0.99**							
Rb	**0.95**								Ba	**0.98**							
Sb	**0.94**								Rb	**0.98**							
Co	**0.94**								Sc	**0.97**							
Sn	**0.91**								Cd	**0.97**							
Hg	**0.91**								Hg	**0.96**							
Cd	**0.91**								Cr	**0.94**							
Sc	**0.90**								Zn	**0.91**							
Cr	0.85								Sb	**0.90**							
Pb	0.84					**0.34**			Ni	**0.90**							**0.37**
Zn	0.83								Cu	0.88							
EC	0.77								Sn	0.81					**0.43**		
Ni	0.63				0.38		**0.53**		BaP		**0.97**						
Cu	0.61							**0.41**	BaA		**0.96**						
OC	0.59								PYR		**0.95**						
FLU		**0.99**							CHR		**0.93**						
ACY		**0.99**							IND		**0.92**						
ANT		**0.98**							FLA		**0.92**						
ACE		**0.98**							BgP		0.89						
PHE		**0.96**							NO_3^-		0.53		0.45				
NAP		**0.94**							ACY			**0.97**					
IND		0.66		0.56					FLU			**0.97**					
Fe			**0.83**						ANT			**0.97**					
K^+			**0.83**			**0.32**			NAP			**0.95**					
Mg			**0.83**						ACE			**0.95**					
Si			**0.81**						PHE			**0.95**					
Ca^+			**0.80**						Mg				**0.96**				
Al			**0.74**						Si				**0.93**				
Na^+			0.56		0.39				Al				**0.91**				
Cl^-			0.56			**0.46**			Ca^+				**0.86**				
FLA				**0.92**					Fe				**0.78**				
BaA				**0.89**					K^+				0.65	0.41		**0.51**	
PYR				**0.87**					Na^+				0.61	0.36			
CHR				**0.72**					NH_4^+					**0.91**			
BgP		0.42		0.62			0.46		SO_4^{2-}					**0.90**			
BkF		0.45		0.60		0.54			Cl^-		0.33				**0.79**		
NH_4^+					**0.97**				Pb	0.41					**0.79**		
SO_4^{2-}					**0.96**				BkF				0.35				
NO_3^-						**0.81**			OC							**0.81**	
BaP		0.36		0.33		**0.76**			EC							**0.79**	
V					0.59		**0.70**		As								
As			0.34					**0.57**	V								**0.82**
Variance (%)	29.9	16.9	14.1	10.6	6.85	5.62	3.92	2.86		26.6	17.0	14.7	13.9	5.80	5.69	5.09	3.27
Cumulative variance (%)	29.9	46.8	60.9	71.5	78.4	84.0	87.9	90.8		26.6	43.6	58.3	72.2	78.0	83.7	88.8	92.1

[a] Rotation method: Varimax standardization with Kaiser. The largest species loadings are presented in bold.

Table 8. Principal component analysis (PCA[a]) for $PM_{2.5}$ samples at the Jasso (JAS) and Tepeji (TEP) sites during 2006. Rotation method: Varimax standardization with Kaiser.

	JAS						TEP				
	Cement kiln	Soil and Fugitive dust	Oil combustion	Biomass combustion	Industry		Cement kiln	Soil and Fugitive dust	Oil combustion	Industry	Biomass combustion
Ba	**0.97**					Co	**0.99**				
Co	**0.96**					Cd	**0.98**				
Sb	**0.94**					Hg	**0.97**				
Sn	**0.92**					Ba	**0.96**				
Hg	**0.90**					Cr	**0.91**				
Cd	**0.90**					Sb	**0.90**			0.35	
Zn	**0.87**					Zn	**0.88**			0.35	0.22
Cr	**0.86**					Cu	**0.87**				
Pb	**0.82**			**0.38**		Ni	**0.84**		**0.42**		
EC	**0.66**	0.30	0.25			Sn	**0.76**			0.55	
OC	**0.58**	0.47				Mg		**0.95**			
Fe		**0.95**				Si		**0.95**			
Si		**0.93**				Al		**0.94**			
Mg		**0.88**				Ca^+		**0.91**			
Al		**0.88**				Fe		**0.77**			
Ca^+		**0.79**	0.29			Na^+		0.60	0.43		
K^+		0.61		**0.57**		NO_3^-		0.55	0.33	**0.54**	
SO_4^{2-}			**0.95**			SO_4^{2-}			**0.94**		
NH_4^+			**0.94**			NH_4^+			**0.94**		
V			**0.88**			V			**0.79**		
S		0.35	0.77			S	0.41		0.72		0.22
Ni	0.57		**0.72**			Cl^-				**0.87**	
Cl^-				**0.75**		Pb	0.38			**0.83**	
NO_3^-				**0.75**		OC	0.20	0.26			**0.82**
Na^+			0.40	0.49	0.44	EC	0.28				**0.79**
Cu	0.47				**0.73**	K^+		0.52	0.38		**0.67**
Variance (%)	35.6	21.7	15.9	8.0	4.5		36.3	20.5	13.8	9.10	8.10
Cumulative variance (%)	35.6	57.3	73.2	81.2	85.7		36.3	56.8	70.6	79.7	87.8

[a] Rotation method: Varimax standardization with Kaiser. The largest species loadings are presented in bold.

quarries, particularly at JAS (Sharma and Pervez, 2004). The fourth factor (9–13% of variance) represents biomass burning. This factor was mainly associated with K^+, along with As, Rb, NO_3^-, and Zn (Hedberg *et al.*, 2005; Manousakas *et al.*, 2017; Lin *et al.*, 2018; Wang *et al.*, 2020). The fifth factor (8%) in TEP is related to cooking activities. The presence of OC could be attributed to the fumes emitted from the oil-based cooking, whereas SO_4^{2-} and NO_3^- could be related to fuel combustion (Sun *et al.*, 2020). The presence of Na^+ has been associated with salts used in cooking (Sun *et al.*, 2020). In JAS, the fifth factor (14%) was related to secondary inorganic aerosols characterized by NH_4^+, SO_4^{2-}, and NO_3^- (Khan *et al.*, 2021). These elements may trace vehicular and industrial emissions, which undergo atmospheric transport and transformations from gas to particle (Liu *et al.*, 2017). The sixth factor (6–10%) is associated with industrial emissions. Pb, Cr, and Sb can be released by cement plant and metal manufacturing processes in TEP (Taiwo *et al.*, 2014; Hua *et al.*, 2016), while Cr, Co, NO_3^-, and Cl^- may originate from waste incinerator plants and metal industries in JAS (Taiwo *et al.*, 2014; Liu *et al.*, 2017; Lucarelli *et al.*, 2019).

Separation of a mixture of pollution sources presents a challenge for factor analysis methods, including PCA and Positive Matrix Factorization (PMF) owing to profile mixing when measured compounds are highly correlated (Watson *et al.*, 2016). Vehicle engine exhaust is clearly identified

Table 9. Principal component analysis (PCA[a]) for $PM_{2.5}$ samples at the Jasso (JAS) and Tepeji (TEP) sites during 2011.

	Jasso							Tepeji					
	Oil combustion	Soil and Fugitive dust	Secondary aerosols	Traffic	Industry	Biomass combustion		Oil combustion	Traffic	Soil and Fugitive dust	Biomass combustion	Cooking activities	Industry
Ni	**0.95**						V	**0.88**					
V	**0.94**						Mo	**0.86**					
Mo	**0.93**						Ca^+	**0.85**					
Sn	**0.83**	0.34					Ni	**0.82**		0.32			
Pb	**0.73**	0.57					NH_4^+	**0.81**					
Zn	**0.69**					**0.44**	SO_4^{2-}	**0.76**			0.43	**0.32**	
Al		**0.82**					K^+	0.62			**0.53**		
Ca^+	0.39	**0.77**		0.29			Ba	0.59		0.32			**0.38**
Mg		**0.75**					Zn		**0.87**				
Ba		**0.75**					Sn		**0.86**				
Sb	0.41	**0.71**		0.35			Sb		**0.79**				**0.35**
Si	0.41	**0.65**	0.40	0.35	0.32		Cd		**0.73**				
Fe	0.48	**0.64**	0.39		0.29		Fe		**0.63**	0.56			
NH_4^+			**0.94**				EC		**0.61**				
SO_4^{2-}			**0.93**				Al		0.59	0.55			
Cd	0.56		**0.74**				OC	0.40	0.53			**0.47**	
NO_3^-	0.38		**0.64**		**0.46**		Si		0.41	**0.85**			
Rb			**0.63**			**0.54**	Mg	0.38		**0.81**			
Cu		0.31		**0.90**			Na^+			**0.77**		**0.33**	
OC				**0.88**		0.22	Co	0.58		**0.64**			
Cl^-				**0.81**	**0.43**		Cr			0.59			**0.39**
EC	0.22			**0.74**			Cl^-		0.47	0.57			
As		0.44					As				**0.91**		
Cr					**0.91**		Rb				**0.89**		
Co					**0.64**	0.48	NO_3^-		0.36		**0.74**	**0.36**	
K^+			0.24			**0.75**	Cu						
Na^+		0.31			0.31		Pb		0.49				**0.70**
Variance (%)	21.3	17.6	14.4	13.4	9.63	9.10		22.1	19.2	16.5	13.0	7.5	5.8
Cumulative variance (%)	21.3	38.9	53.3	66.7	76.3	85.4		22.1	41.3	57.8	70.8	78.3	84.1

[a] Rotation method: Varimax standardization with Kaiser. The largest species loadings are presented in bold.

with the inclusion of PAHs, along with a higher percentage (91–92%) of variance explained (Table 7). Other factors contributing to air pollution at TIC for the 2006 and 2011 samples includes cement kiln emissions with heavy-oil and recycled alternative-fuel combustion, biomass burning, metal industry, and fugitive dust.

3.5. Health Risk Assessment

A health risk assessment was conducted with average As, Cd, Co, Cr (VI), Ni, and Pb, concentrations representing carcinogenic elements in $PM_{2.5}$ (Table 10). Pb had the highest exposure concentration for both children and adults in 2006, while Ni exhibited the highest exposure concentration (ExCo) in 2010–2011. These two elements did not exceed the acceptable level of carcinogenic risk of one in 10,000 population (1×10^{-4}) (U.S. EPA, 2011) during the study period. However, Cr concentrations exceeded the minimal acceptable risk level (1×10^{-6}) in 2006 (U.S. EPA, 2011), registering the highest ICR values in TEP (1.3×10^{-5} for children and 5.3×10^{-5} for adults). Although ICR values for Cr were reduced from 2006 to 2010/2011, especially for children in JAS (6.1×10^{-7}), but Cr remained to pose critical health risk. Similar results have been

Table 10. Carcinogenic risks by the inhalation of selected toxic $PM_{2.5}$ elements in Jasso (JAS) and Tepeji (TEP) during 2006 and 2010/2011.

Element	JAS (2006)				TEP (2006)			
	ExCo (μg m^{-3})		Individual Cancer Risk		ExCo (μg m^{-3})		Individual Cancer Risk	
	Children	Adults	Children	Adults	Children	Adults	Children	Adults
Cr	1.6E-04	6.4E-04	**1.9E-06**	**7.6E-06**	1.1E-03	4.5E-03	**1.3E-05**	**5.3E-05**
Co	3.4E-05	1.4E-04	2.6E-07	**1.1E-06**	3.4E-05	1.4E-04	2.6E-07	**1.1E-06**
Ni	8.0E-04	3.2E-03	1.9E-07	7.7E-07	7.1E-04	2.9E-03	1.7E-07	6.9E-07
As	2.1E-05	8.3E-05	6.8E-08	2.7E-07	1.8E-05	7.0E-05	5.8E-08	2.3E-07
Cd	5.9E-04	2.3E-03	**1.1E-06**	**4.2E-06**	6.0E-04	2.4E-03	**1.1E-06**	**4.3E-06**
Pb	1.5E-03	6.0E-03	1.8E-08	7.2E-08	1.5E-02	6.1E-02	1.8E-07	7.3E-07
Sum	3.1E-03	1.2E-02	3.5E-06	1.4E-05	1.8E-02	7.1E-02	1.5E-05	6.0E-05
Element	JAS (2010/2011)				TEP (2010/2011)			
	ExCo (μg m^{-3})		Individual Cancer Risk		ExCo (μg m^{-3})		Individual Cancer Risk	
	Children	Adults	Children	Adults	Children	Adults	Children	Adults
Cr	5.1E-05	2.0E-04	6.1E-07	**2.4E-06**	8.4E-05	3.4E-04	**1.0E-06**	**4.1E-06**
Co	8.4E-06	3.4E-05	6.6E-08	2.6E-07	4.6E-06	1.8E-05	3.6E-08	1.4E-07
Ni	4.7E-04	1.9E-03	1.1E-07	4.5E-07	6.8E-04	2.7E-03	1.6E-07	6.5E-07
As	8.4E-06	3.4E-05	2.8E-08	1.1E-07	5.1E-05	2.0E-04	1.7E-07	6.7E-07
Cd	2.3E-05	9.2E-05	4.1E-08	1.7E-07	1.7E-05	6.8E-05	3.0E-08	1.2E-07
Pb	2.2E-04	8.8E-04	2.7E-09	1.1E-08	4.8E-04	1.9E-03	5.8E-09	2.3E-08
Sum	7.8E-04	3.1E-03	8.6E-07	3.4E-06	1.3E-03	5.3E-03	1.4E-06	5.7E-06

Table 11. Benzo[a]pyrene (BaP) equivalent concentration and the inhalation life-time cancer risk.

Sampling site	BaP_{eq} (ng m^{-3})	ILCR
JAS	1.34	1.2×10^{-4}
TEP	0.99	8.6×10^{-5}

reported in areas influenced by industrial emissions (Cheng *et al.*, 2017; Liu *et al.*, 2018; Ramírez *et al.*, 2020).

The ICR values for Cd (for both children and adults) and Co (only for adults) were also slightly higher than the minimal acceptable risk level, ranging between 1.1×10^{-6} and 4.3×10^{-6} in 2006 (Table 10). However, exposure concentrations of Cd and Co were noticeably reduced during 2010/2011, resulting in negligible values of carcinogenic risk (below 1×10^{-6}) (U.S. EPA, 2011). Overall, the total cancer risk decreased for both children and adults in 2010/2011 (between 3.5×10^{-6} and 6.0×10^{-5}) compared to 2006 (between 8.6×10^{-7} and 5.7×10^{-6}), which reflects the health benefits from switching of fuel oil to natural gas in the power plant.

BaP_{eq}, a parameter used to evaluate the human health risk (Shen *et al.*, 2019), exhibited 35% higher value in JAS as compared to TEP (Table 11). These BaP_{eq} values (0.99–1.34 ng m^{-3}) are similar to those measured in Shanghai during winter (0.916–1.86 ng m^{-3}) (Yang *et al.*, 2021), but higher than values found in cities of Pakistan (< 0.24 ng m^{-3}) (Ishtiaq *et al.*, 2021). Average BaP_{eq} in TIC were lower than that reported in northern China during winter (3.16–120 ng m^{-3}) (Shen *et al.*, 2019) and in Islamabad (5.19–10.61 ng m^{-3}) (Mehmood *et al.*, 2020). Average BaP_{eq} of 1.34 ng m^{-3} in JAS was above the standard of 1 ng m^{-3} defined by WHO, representing a health risk for the exposed population.

In addition, the ILCR was 8.6×10^{-5} and 1.2×10^{-4} at TEP and JAS (Table 11), respectively, indicating ~9 cancer cases can occur per 100,000 inhabitants at TEP and 2 cases can occur per 10,000 inhabitants at JAS. Both ILCR values exceeded the threshold value (1×10^{-6}) suggested by U.S. EPA, but the risk in JAS stands out since it is two orders of magnitude higher than the U.S. EPA acceptable cancer risk level. The results suggest the importance of periodically monitoring the risk by inhalation of atmospheric PAHs in the TIC.

3 CONCLUSIONS

This study characterized over ~320 $PM_{2.5}$ mass and chemical composition samples acquired at the two Central Mexico Tula Industrial Corridor sites (Jasso [JAS] and Tepeji [TEP] during the dry-warm months (March–May) in 2006, 2010, and 2011. A decreasing trend was found for $PM_{2.5}$ mass with 30% and 19% reduction from 2006 to 2010 at the JAS and TEP sites, respectively. $PM_{2.5}$ mass in 2006 were 31.03 ± 0.93 μg m^{-3} (JAS) and 25.72 ± 0.26 μg m^{-3} (TEP), consisting of 47–57% of carbonaceous aerosol (OC × 1.4 + EC) and 40–44% of ionic species demonstrated by SO_4^{2-}. While most of the SO_4^{2-} was in the form of ammonium sulfate, the ion balance showed that there was not enough NH_4^+ to neutralize SO_4^{2-}, suggesting the presence of ammonium bisulfate and sulfuric acid of nearby origin.

The sum of the 15 PAHs ranged from 14–18 μg m^{-3}, lower than the 50–310 μg m^{-3} range reported in Mexico City and orders of magnitude lower than those found in U.S.A., China, India, and Spain. Geological minerals contributed ~8–10% of $PM_{2.5}$ mass with abundant (> 60%) Ca in JAS, attributing to nearby limestone mining and quarries.

Air pollution concentrations were reduced from 2006 to 2010/2011 as a result of implementing air pollution control measures, such as the substitution of industrial fuel to natural gas that reduces industrial emissions and minimize health risks of the exposed population. Thus, the cancer risk of toxic trace elements in 2010/2011 was reduced by an order of magnitude relative to 2006. However, it is crucial to monitor the health risk from inhalation of PAHs, especially in JAS where a higher risk was found.

This study showed that heavy-oil combustion and vehicle engine exhaust are major sources of $PM_{2.5}$. Therefore, it is necessary to use cleaner fuels to improve air quality. Implementing control measures at the TIC would lead to less transport downwind that impact Mexico City and the State of Mexico.

Although $PM_{2.5}$ concentrations at JAS and TEP during the study periods were within the Mexican National Ambient Air Quality Standard, it is recommended to continuously monitor the chemical composition and conducts source apportionment of $PM_{2.5}$, since elevated PAHs and toxic compounds such as Cd, Cr, and Pb consistently posing health risks.

ACKNOWLEDGEMENTS

The authors gratefully acknowledge the support of PEMEX for fieldwork under contract IMP-UAJ-DC-018-2006. Additional support for the writing of the manuscript is provided by the UNAM-funded project PAPIIT IA100809.

DISCLAIMER

Reference to any companies or specific commercial products does not constitute an endorsement by the authors.

SUPPLEMENTARY MATERIAL

Supplementary material for this article can be found in the online version at https://doi.org/10.4209/aaqr.210047

REFERENCES

Ahmad, M., Rihawy, M.S., Haydr, R., Tlass, M., Roumie, M., Srour, A. (2020). PIXE and statistical analysis of fine airborne particulate matter ($PM_{2.5}$) in Damascus. Nucl. Instrum. Methods Phys. Res. B 462, 75–81. https://doi.org/10.1016/j.nimb.2019.11.003

Almanza, V.H., Molina, L.T., Sosa, G. (2012). Soot and SO_2 contribution to the supersites in the MILAGRO campaign from elevated flares in the Tula Refinery. Atmos. Chem. Phys. 12, 10583–

10599. https://doi.org/10.5194/acp-12-10583-2012

Alvarez-Ospina, H., Giordano, S., Ladino, L., Raga, G., Muñoz-Salazar, J., Leyte-Lugo, M., Rosas, D., Carabali, G. (2021). Particle-bound polycyclic aromatic hydrocarbons (pPAHs) in Merida, Mexico. Aerosol Air Qual. Res. 21, 200245. https://doi.org/10.4209/aaqr.200245

Amador-Muñoz, O., Villalobos-Pietrini, R., Miranda, J., Vera-Avila, L.E. (2011). Organic compounds of $PM_{2.5}$ in Mexico Valley: Spatial and temporal patterns, behavior and sources. Sci. Total Environ. 409, 1453–1465. https://doi.org/10.1016/j.scitotenv.2010.11.026

Amador-Muñoz, O., Martínez-Domínguez, Y.M., Gómez-Arroyo, S., Peralta, O. (2020). Current situation of polycyclic aromatic hydrocarbons (PAH) in $PM_{2.5}$ in a receptor site in Mexico City and estimation of carcinogenic PAH by combining non-real-time and real-time measurement techniques. Sci. Total Environ. 703, 134526. https://doi.org/10.1016/j.scitotenv.2019.134526

Arfala, Y., Douch, J., Assabbane, A., Kaaouachi, K., Tian, H., Hamdani, M. (2018). Assessment of heavy metals released into the air from the cement kilns co-burning waste: Case of Oujda cement manufacturing (Northeast Morocco). Sustain. Environ. Res. 28, 363–373. https://doi.org/10.1016/j.serj.2018.07.005

Bernardoni, V., Vecchi, R., Valli, G., Piazzalunga, A., Fermo, P. (2011). PM_{10} source apportionment in Milan (Italy) using time-resolved data. Sci. Total Environ. 409, 4788–4795. https://doi.org/10.1016/j.scitotenv.2011.07.048

Camacho-López, C., Marmolejo-Santillán, Y., Otazo-Sánchez, E., Romo-Gómez, C. (2019). Emisiones de GEI del corredor industrial Apaxco-Tula. Publicación Semestral Pädi 13, 12–16. https://doi.org/10.29057/icbi.v7i13.3443

Cangialosi, F., Intini, G., Liberti, L., Notarnicola, M., Stellacci, P. (2008). Health risk assessment of air emissions from a municipal solid waste incineration plant – A case study. Waste Manage. 28, 885–895. https://doi.org/10.1016/j.wasman.2007.05.006

Castro, L.M., Pio, C.A., Harrison, R.M., Smith, D.J.T. (1999). Carbonaceous aerosol in urban and rural European atmospheres: Estimation of secondary organic carbon concentrations. Atmos. Environ. 33, 2771–2781. https://doi.org/10.1016/S1352-2310(98)00331-8

Chen, J., Gao, M., Li, D., Li, L., Song, M., Xie, Q. (2021). Changes in $PM_{2.5}$ emissions in China: An extended chain and nested refined laspeyres index decomposition analysis. J. Cleaner Prod. 294, 126248. https://doi.org/10.1016/j.jclepro.2021.126248

Chen, Y.C., Chiang, H.C., Hsu, C.Y., Yang, T.T., Lin, T.Y., Chen, M.J., Chen, N.T., Wu, Y.S. (2016). Ambient $PM_{2.5}$-bound polycyclic aromatic hydrocarbons (PAHs) in Changhua County, central Taiwan: Seasonal variation, source apportionment and cancer risk assessment. Environ. Pollut. 218, 372–382. https://doi.org/10.1016/j.envpol.2016.07.016

Cheng, X., Huang, Y., Long, Z., Ni, Sh., Shi, Z., Zhang, C. (2017). Characteristics, sources and health risk assessment of trace metals in PM_{10} in Panzhihua, China. Bull. Environ. Contam. Toxicol. 98, 76–83. https://doi.org/10.1007/s00128-016-1979-0

ChooChuay, C., Pongpiachan, S., Tipmanee, D., Suttinun, O., Deelaman, W., Wang, Q., Xing, L., Li, G., Han, Y., Palakun, J., Cao, J. (2020). Impacts of $PM_{2.5}$ sources on variations in particulate chemical compounds in ambient air of Bangkok, Thailand. Atmos. Pollut. Res. 11, 1657–1667. https://doi.org/10.1016/j.apr.2020.06.030

Chow, J. (1995). Measurement methods to determine compliance with ambient air quality standards for suspended particles. J. Air Waste Manage. Assoc. 45, 320–382. https://doi.org/10.1080/10473289.1995.1046739

Chow, J.C., Watson, J.G., Pritchett, L.C., Pierson, W.R., Frazier, C.A., Purcell, R.G., (1993). The dri thermal/optical reflectance carbon analysis system: Description, evaluation and applications in U.S. Air quality studies. Atmos. Environ. 27, 1185–1201. https://doi.org/10.1016/0960-1686(93)90245-T

Chow, J.C., Watson, J.G., Crow, D., Lowenthal, D.H., Merrifield, T. (2001). Comparison of IMPROVE and NIOSH carbon measurements. Aerosol Sci. Technol. 34, 1–12. https://doi.org/10.1080/02786820119073

Chow, J.C., Watson, J.G., Edgerton, S.A., Vega, E. (2002). Chemical composition of $PM_{2.5}$ and PM_{10} in Mexico City during winter 1997. Sci. Total Environ. 287, 177–201. https://doi.org/10.1016/S0048-9697(01)00982-2

Chow, J.C., Watson, J.G., Chen, L.W.A., Chang, M.C.O., Robinson, N.F., Trimble, D.L., Kohl, S.D. (2007). The IMPROVE_A temperature protocol for thermal/optical carbon analysis: Maintaining

consistency with a long-term database. J. Air Waste Manage. Assoc. 57, 1014–1023. https://doi.org/10.3155/1047-3289.57.9.1014

Chow, J.C., Lowenthal, D.H., Chen, L.W.A., Wang, X., Watson, J.G. (2015). Mass reconstruction methods for $PM_{2.5}$: A review. Air Qual. Atmos. Health 8, 243–263. https://doi.org/10.1007/s11869-015-0338-3

Corbin, J., Mensah, A., Pieber, S., Orasche, J., Michalke, B., Zanatta, M., Czech, H., Massabò, D., Buatier de Mongeot, F., Mennucci, C., El Haddad, I., Kumar, N., Stengel, B., Huang, Y., Zimmermann, R., Prévôt, A.S.H., Gysel, M. (2018). Trace metals in soot and $PM_{2.5}$ from heavy-fuel-oil combustion in a marine engine. Environ. Sci. Technol. 52, 6714–6722. https://doi.org/10.1021/acs.est.8b01764

Das, R., Taufiq, A., Rakshit, D., Shome, D., Wang, X. (2018). Sources of atmospheric lead (Pb) in and around an Indian megacity. Atmos. Environ. 193, 57–65. https://doi.org/10.1016/j.atmosenv.2018.08.062

Diario Oficial de la Federación (DOF) (2004). Protección ambiental-Fabricación de cemento hidráulico-Niveles máximos permisibles de emisión a la atmósfera NOM-040-SEMARNAT-2002. http://dof.gob.mx/nota_detalle.php?codigo=677963&fecha=20/04/2004

Du, Y., Xu, X., Chu, M., Guo, Y., Wang, J. (2016). Air particulate matter and cardiovascular disease: The epidemiological, biomedical and clinical evidence. J. Thorac. Dis. 8, E8–E19. https://doi.org/10.3978/j.issn.2072-1439.2015.11.37

Duan, X., Yan, Y., Li, R., Deng, M., Hu, D., Peng, L. (2021). Seasonal variations, source apportionment, and health risk assessment of trace metals in $PM_{2.5}$ in the typical industrial city of Changzhi, China. Atmos. Pollut. Res. 12, 365–374. https://doi.org/10.1016/j.apr.2020.09.017

Dzepina, K., Arey, J., Marr, L.C., Worsnop, D.R., Salcedo, D., Zhang, Q., Onasch, T.B., Molina, L.T., Molina, M.J., Jimenez, J.L. (2007). Detection of particle-phase polycyclic aromatic hydrocarbons in Mexico City using an aerosol mass spectrometer. Int. J. Mass Spectrom. 263, 152–170. https://doi.org/10.1016/j.ijms.2007.01.010

Eiguren-Fernandez, A., Miguel, A.H., Froines, J.R., Thurairatnam, S., Avol, E.L. (2004). Seasonal and spatial variation of polycyclic aromatic hydrocarbons in vapor-phase and $PM_{2.5}$ in Southern California urban and rural communities. Aerosol Sci. Technol. 38, 447–455. https://doi.org/10.1080/02786820490449511

Fadel, M., Ledoux, F., Farhat, M., Kfoury, A., Courcot, D., Afif, C. (2021). $PM_{2.5}$ characterization of primary and secondary organic aerosols in two urban-industrial areas in the East Mediterranean. J. Environ. Sci. 101, 98–116. https://doi.org/10.1016/j.jes.2020.07.030

García-Escalante, J., García-Reynoso, J., Jazcilevich-Diamant, A., Ruiz-Suárez, L. (2014). The influence of the Tula, Hidalgo complex on the air quality of the Mexico City Metropolitan Area. Atmósfera 27, 215–225. https://doi.org/10.1016/S0187-6236(14)71111-7

Gobierno de Mexico (2019). Informa Conapo sobre la esperanza de vida de la población mexicana. https://www.gob.mx/segob/prensa/informa-conapo-sobre-la-esperanza-de-vida-de-la-poblacion-mexicana (accessed 10 October 2020).

Gonzalez, L., Longoria, F.E., Sanchez-Domínguez, M., Leyva-Porras, C., Silva-Vidaurri, L.G., Acuna-Askar, K., Kharisov, B.I., Villarreal, J.F., Alfaro, J.M. (2016). Chemical and morphological characterization of TSP and $PM_{2.5}$ by SEM-EDS, XPS and XRD collected in the metropolitan area of Monterrey, Mexico. Atmos. Environ. 143, 249–260. https://doi.org/10.1016/j.atmosenv.2016.08.053

Gupta, R., Majumdar, D., Trivedi, J., Bhanarkar, A. (2012). Particulate matter and elemental emissions from a cement kiln. Fuel Process. Technol. 104, 343–351. https://doi.org/10.1016/j.fuproc.2012.06.007

Ha, S., Hu, H., Roussos-Ross, D., Haidong, K., Roth, J., Xu, X. (2014). The effects of air pollution on adverse birth outcomes. Environ. Res. 134, 198–204. https://doi.org/10.1016/j.envres.2014.08.002

Hagino, H., Oyama, M., Sasaki, S. (2016). Laboratory testing of airborne brake wear particle emissions using a dynamometer system under urban city driving cycles. Atmos. Environ. 131, 269–278. https://doi.org/10.1016/j.atmosenv.2016.02.014

Han, Y.M., Du, P.X., Cao, J.J., Posmentier, E.S. (2006). Multivariate analysis of heavy metal contamination in urban dusts of Xi'an, Central China. Sci. Total Environ. 355, 176–186. https://doi.org/10.1016/j.scitotenv.2005.02.026

Hedberg, E., Gidhagen, L., Johansson, C. (2005). Source contributions to PM_{10} and arsenic concentrations in Central Chile using positive matrix factorization. Atmos. Environ. 39, 549–561. https://doi.org/10.1016/j.atmosenv.2004.11.001

Herrera, J., Campos, A., García, F., Blanco, S., Cárdenas, B., Mizohata, A. (2012). Chemical composition of $PM_{2.5}$ particles in Salamanca, Guanajuato Mexico: Source apportionment with receptor models. Atmos. Res. 107, 31–41. https://doi.org/10.1016/j.atmosres.2011.12.010

Hsu, Ch., Chiang, H., Lin, Sh., Chen, M., Lin, T., Chen, Y. (2016). Elemental characterization and source apportionment of PM_{10} and $PM_{2.5}$ in the western coastal area of central Taiwan. Sci. Total Environ. 541, 1139–1150. https://doi.org/10.1016/j.scitotenv.2015.09.122

Hua, S., Tian, H., Wang, K., Zhu, Ch., Gao, J., Ma, Y., Xue, Y., Wang, Y., Duan, Sh., Zhou, J. (2016). Atmospheric emission inventory of hazardous air pollutants from China's cement plants: Temporal trends, spatial variation characteristics and scenario projections. Atmos. Environ. 128, 1–9. https://doi.org/10.1016/j.atmosenv.2015.12.056

Hussar, E., Richards, S., Lin, Z.Q., Dixon, R., Johnson, K. (2013). Human Health Risk Assessment of 16 Priority Polycyclic Aromatic Hydrocarbons in Soils of Chattanooga, Tennessee, USA. Water Air Soil Pollut. 223, 5535–5548. https://doi.org/10.1007/s11270-012-1265-7

Instituto Nacional de Ecología y Cambio Climático (INECC) (2017). Programa de Gestión Federal para Mejorar la Calidad del Aire de la Megalópolis, PROAIRE 2017-2030. INECC/Semarnat, México.

International Agency for Research on Cancer (IARC) (1990). Chromium (III) Compounds. vol. 49. WHO, Lyon.

International Agency for Research on Cancer (IARC) (2006a). Cobalt in Hard Metals and Cobalt Sulfate, Gallium Arsenide, Indium Phosphide and Vanadium Pentoxide. vol. 86. WHO, Lyon.

International Agency for Research on Cancer (IARC) (2006b). Inorganic and Organic Lead Compounds. vol. 87. WHO, Lyon.

International Agency for Research on Cancer (IARC) (2012). Arsenic, Metals, Fibres and Dusts. A Review of Human Carcinogens. vol. 100C. WHO, Lyon.

Inventario de Emisiones del Estado de Hidalgo (IEEH) (2011). Secretaría de Medio Ambiente y Recursos Naturales del Estado de Hidalgo. Hidalgo, México. 2016.

Ishtiaq, J., Hussain, J. Azeem, W., Hamid, N., Jamshed, M., Shahnawaz, M., Nasir, J., Hussain, S., Chakraborty, P., Li, J., Zhang, G. (2021). Atmospheric polycyclic aromatic hydrocarbons (PAHs) at urban settings in Pakistan: Spatial variations, sources and health risks. Chemosphere 274, 129811. https://doi.org/10.1016/j.chemosphere.2021.129811

Jacott, M., Taylor, A., Winfield, M. (2003). Energy use in the cement industry in North America: Emissions, waste generation and pollution control, 1990-2001. Commission for Environmental Cooperation, 2nd ed. North American Symposium on Assessing the Environmental Effects of Trade.

Jedrychowski, W.A., Perera, F.P., Camann, D., Spengler, J., Butscher, M., Mroz, E., Majewska, R., Flak, E., Jacek, R., Sowa, A. (2015). Prenatal exposure to polycyclic aromatic hydrocarbons and cognitive dysfunction in children. Environ. Sci. Pollut. Res. 22, 3631–3639. https://doi.org/10.1007/s11356-014-3627-8

Johnson, K.S., de Foy, B., Zuberi, B., Molina, L.T., Molina, M.J., Xie, Y., Laskin, A., Shutthanandan, V. (2006). Aerosol composition and source apportionment in the Mexico City Metropolitan Area with PIXE/PESA/STIM and multivariate analysis. Atmos. Chem. Phys. 6, 4591–4600. https://doi.org/10.5194/acp-6-4591-2006

Kwiatkowski, S., Polat, M., Yu, W., Stanley, M. (2021). Industrial emissions control technologies: Introduction. in: Goodsite, M.E., Johnson, M.S., Hertel, O. (Eds.), Air pollution sources, statistics, and health effects. Encyclopedia of Sustainability Science and Technology Series. Springer, New York, NY.

Ladino, L., Raga, G., Baumgardner, D. (2018). On particle-bound polycyclic aromatic hydrocarbons (PPAH) and links to gaseous emissions in Mexico City. Atmos. Environ.t 194, 31–40. https://doi.org/10.1016/j.atmosenv.2018.09.022

Lee, B., Kim, B., Lee, K. (2014). Air pollution exposure and cardiovascular disease. Toxicol. Res. 30, 71–75. https://doi.org/10.5487/TR.2014.30.2.071

Lin, Y., Hsu, S., Lin, Ch., Lin, S., Huang, Y., Chang, Y., Zhang, Y. (2018). Enhancements of airborne particulate arsenic over the subtropical free troposphere: Impact of southern Asian biomass

burning. Atmos. Chem. Phys. 18, 13865–13879. https://doi.org/10.5194/acp-18-13865-2018

Liu, B., Wu, J., Zhang, J., Wang, L., Yang, J., Liang, D., Dai, Q., Bi, X., Feng, Y., Zhang, Y., Zhang, Q. (2017). Characterization and source apportionment of $PM_{2.5}$ based on error estimation from EPA PMF 5.0 model at a medium city in China. Environ. Pollut. 222, 10–22. https://doi.org/10.1016/j.envpol.2017.01.005

Liu, K., Shang, Q., Wan, C. (2018). Sources and health risks of heavy metals in $PM_{2.5}$ in a campus in a typical suburb area of Taiyuan, North China. Atmosphere 9, 46. https://doi.org/10.3390/atmos9020046

Lucarelli, F., Barrera, V., Becagli, S., Chiari, M., Giannoni, M., Nava, S., Traversi, R., Calzolai, G. (2019). Combined use of daily and hourly data sets for the source apportionment of particulate matter near a waste incinerator plant. Environ. Pollut. 247, 802–811. https://doi.org/10.1016/j.envpol.2018.11.107

Manchanda, C., Kumar, M., Singh, V., Faisal, M., Hazarika, N., Shukla, A., Lalchandani, V., Goel, V., Thamban, N., Ganguly, D., Tripathi, S. (2021). Variation in chemical composition and sources of $PM_{2.5}$ during the COVID-19 lockdown in Delhi. Environ. Int. 153, 106541. https://doi.org/10.1016/j.envint.2021.106541

Manousakas, M., Papaefthymiou, H., Diapouli, E., Migliori, A., Karydas, A., Bogdanovic-Radovic, I., Eleftheriadis, K. (2017). Assessment of $PM_{2.5}$ sources and their corresponding level of uncertainty in a coastal urban area using EPA PMF 5.0 enhanced diagnostics. Sci. Total Environ. 574, 155–164. https://doi.org/10.1016/j.scitotenv.2016.09.047

Marr, L.C., Grogan, L.A., Wohrnschimmel, H., Molina, L.T., Molina, M. J., Smith, T.J., Garshick, E. (2004). Vehicle traffic as a source of particulate polycyclic aromatic hydrocarbon exposure in Mexico City. Environ. Sci. Technol. 38, 2584–2592. https://doi.org/10.1021/es034962s

Martínez-Carrillo, M., Solís, C., Isaac-Olive, K., Andrade, E., Beltrán-Hernández, R., Martínez-Reséndiz, G., Ramírez-Reyes, A., Calvario, C., Lucho-Constantino, C. (2010). Atmospheric elemental concentration determined by Particle-Induced X-ray Emission at Tlaxcoapan in central Mexico, and its relation to Tula industrial-corridor emissions. Microchem. J. 94, 48–52. https://doi.org/10.1016/j.microc.2009.08.011

Mehmood, T., Zhu, T., Ahmad, I., Li, X. (2020). Ambient $PM_{2.5}$ and PM_{10} bound PAHs in Islamabad, Pakistan: Concentration, source and health risk assessment. Chemosphere 257, 127187. https://doi.org/10.1016/j.chemosphere.2020.127187

Mihankhah, T., Saeedi, M., Karbassi, A. (2020). Contamination and cancer risk assessment of polycyclic aromatic hydrocarbons (PAHs) in urban dust from different land-uses in the most populated city of Iran. Ecotoxicol. Environ. Saf. 187, 109838. https://doi.org/10.1016/j.ecoenv.2019.109838

Minocha, A.K., Goyal, M.K. (2013). Immobilization of molybdenum in ordinary Portland cement. J. Chem. Eng. Process. Technol. 4, 1000159. https://doi.org/10.4172/2157-7048.1000162

Montelongo-Reyes, M., Otazo-Sánchez, E.M., Romo-Gómez, C., Gordillo-Martínez, A.J., Galindo-Castillo, E. (2015). GHG and black carbon emission inventories from Mezquital Valley: The main energy provider for Mexico Megacity. Sci. Total Environ. 527–528, 455–464. https://doi.org/10.1016/j.scitotenv.2015.03.129

Muendo, M., Hanai, Y., Kameda, Y., Masunaga, S. (2006). Polycyclic aromatic hydrocarbons in urban air: Concentration levels, patterns, and source analysis in Nairobi, Kenya. Environ. Forensics. 7, 147–157. https://doi.org/10.1080/15275920600667112

Murillo-Tovar, M., Barradas-Gimate, A., Arias-Montoya, M., Saldarriaga-Noreña, H. (2018). Polycyclic Aromatic Hydrocarbons (PAHs) associated with $PM_{2.5}$ in Guadalajara, Mexico: Environmental levels, health risks and possible sources. Environments 5, 62. https://doi.org/10.3390/environments5050062

National Research Council (2000). Toxicological risks of selected flame-retardant chemicals. Subcommittee on Flame-Retardant Chemicals, Committee on Toxicology, Board on Environmental Studies and Toxicology, Washington D.C.

Nirmalkar, J., Haswani, D., Singh, A., Kumar, S., Raman, R. (2021). Concentrations, transport characteristics, and health risks of $PM_{2.5}$-bound trace elements over a national park in central India. J. Environ. Manage. 293, 112904. https://doi.org/10.1016/j.jenvman.2021.112904

Nisbet, I.C., Lagoy, P.K. (1992). Toxic equivalency factors (TEFs) for polycyclic aromatic hydrocarbons (PAHs). Regul. Toxicol. Pharm. 16, 290–300. https://doi.org/10.1016/0273-

2300(92)90009-X

Niu, X., Hang, S., Ho, K., Huang, Y., Sun, J., Wang, Q., Zhou, Y., Zhao, Z., Cao, J. (2017). Atmospheric levels and cytotoxicity of polycyclic aromatic hydrocarbons and oxygenated-PAHs in $PM_{2.5}$ in the Beijing-Tianjin-Hebei region. Environ. Pollut. 231, 1075–1084. https://doi.org/10.1016/j.envpol.2017.08.099

Park, E., Kim, D., Park, K. (2008). Monitoring of ambient particles and heavy metals in a residential area of Seoul, Korea. Environ. Monit. Assess. 137, 441–449. https://doi.org/10.1007/s10661-007-9779-y

Querol, X., Pey, J., Minguillón, M.C., Pérez, N., Alastuey, A., Viana, M., Moreno, T., Bernabé, R.M., Blanco, S., Cárdenas, B., Vega, E., Sosa, G., Escalona, S., Ruiz, H., Artíñano, B. (2008). PM speciation and sources in Mexico during the MILAGRO-2006 Campaign. Atmos. Chem. Phys. 8, 111–128. https://doi.org/10.5194/acp-8-111-2008

Rajput, N., Lakhani, A. (2009). Measurements of polycyclic aromatic hydrocarbons at an industrial site in India. Environ Monit. Assess. 150, 273–284. https://doi.org/10.1007/s10661-008-0229-2

Ramírez, N., Cuadras, A., Rovira, E. Marcé, R.M., Borrull. F. (2011). Risk assessment related to atmospheric polycyclic aromatic hydrocarbons in gas and particle phases near industrial sites. Environ. Health Perspect. 118, 1110–1116. https://doi.org/10.1289/ehp.1002855

Ramírez, O., Sánchez de la Campa, A.M., de la Rosa, J. (2018). Characteristics and temporal variations of organic and elemental carbon aerosols in a high-altitude, tropical Latin American megacity. Atmos. Res. 210, 110–122. https://doi.org/10.1016/j.atmosres.2018.04.006

Ramírez, O., Sánchez de la Campa, A.M., Sánchez-Rodas, D., de la Rosa, J. (2020). Hazardous trace elements in thoracic fraction of airborne particulate matter: Assessment of temporal variations, sources, and health risks in a megacity. Sci. Total Environ. 710, 136344. https://doi.org/10.1016/j.scitotenv.2019.136344

Ravindra, K., Sokhi, R., Van Grieken, R. (2008). Atmospheric polycyclic aromatic hydrocarbons: Source attribution, emission factors and regulation. Atmos. Environ. 42, 2895–2921. https://doi.org/10.1016/j.atmosenv.2007.12.010

Satarug, S., Garrett, S.H., Sens, M.A., Sens, D.A. (2010). Cadmium, environmental exposure, and health outcomes. Environ. Health Perspect. 118, 182–190. https://doi.org/10.1289/ehp.0901234

Semarnat (2008). Evaluación de instrumentos normativos del sector ambiental. http://biblioteca.semarnat.gob.mx/janium/Documentos/Ciga/Libros2011/CD001056.pdf

Semarnat (2010). Tramites-rubro 3. Coprocesamiento de residuos peligrosos industriales. http://app2.semarnat.gob.mx/tramites/index.php?option=com_content&view=article&id=532&Itemid=128

Semarnat (2016). Potencial para la valorización energética de residuos urbanos en México, a través del coprocesamiento en hornos cementeros. Programa Aprovechamiento Energético de Residuos Urbanos en México. https://www.giz.de/en/downloads/giz2016-es-EnRes-Potencial_para_la_valorizacion_energetica.pdf

Sener, Prospectiva de Petróleo Crudo y Petrolíferos 2013-2027, Mexico, 2013.

Sharma, R., Pervez, S. (2004). Chemical characterization and enrichment of selected toxic elements in ambient particulate matter around a slag-based cement plant in Chhattisgarh state - A case study. J. Sci. Ind. Res. 63, 376–382. http://nopr.niscair.res.in/handle/123456789/5424

Shen, R., Wang, Y., Gao, W., Cong, X., Cheng, L., Li, X. (2019). Size-segregated particulate matter bound polycyclic aromatic hydrocarbons (PAHs) over China: Size distribution, characteristics and health risk assessment. Sci. Total Environ. 685, 116–123. https://doi.org/10.1016/j.scitotenv.2019.05.436

Silva, L.F.O., Schneider, I.L., Artaxo, P., Núñez-Blanco, Y., Pinto, D., Flores, É.M.M., Gómez-Plata, L., Ramírez, O., Dotto, G.L. (2020). Particulate matter geochemistry of a highly industrialized region in the Caribbean: Basis for future toxicological studies. Geosci. Front. 101115. https://doi.org/10.1016/j.gsf.2020.11.012

Sosa, E.R., Vega, E., Wellens, A., Jaimes, M., Fuentes, G.G., Granados, H.E., Alarcón, J.A., Torres, B.M., Sánchez, A.P., Rosas, A.S., Mateos, D.E. (2020). Reduction of atmospheric emissions due to switching from fuel oil to natural gas at a power plant in a critical area in Central Mexico. J. Air Waste Manage. Assoc. 70, 1043–1059. https://doi.org/10.1080/10962247.2020.1808113

Sosa, G., Vega, E., González-Avalos, E., Mora, V., López-Veneroni, D. (2013). Air pollutant characterization in Tula industrial corridor, Central Mexico, during the MILAGRO study.

BioMed Res. Int. 2013, 521728. https://doi.org/10.1155/2013/521728

Sun, S., Shi, W., Tang, Y., Han, Y., Du, X., Zhou, W., Zhang, W., Sun, C., Liu, G. (2021). The toxic impacts of microplastics (MPs) and polycyclic aromatic hydrocarbons (PAHs) on haematic parameters in a marine bivalve species and their potential mechanisms of action. Sci. Total Environ. 783, 147003. https://doi.org/10.1016/j.scitotenv.2021.147003

Taiwo, A., Harrison, R., Shi, Z. (2014). A review of receptor modelling of industrially emitted particulate matter. Atmos. Environ. 97, 109–120. https://doi.org/10.1016/j.atmosenv.2014.07.051

Thornhill, D.A., de Foy, B., Herndon, S.C., Onasch, T.B., Wood, E.C., Zavala, M., Molina, L.T., Gaffney, J.S., Marley, N.A., Marr, L.C. (2008). Spatial and temporal variability of particulate polycyclic aromatic hydrocarbons in Mexico City, Atmos. Chem. Phys. 8, 3093–3105. https://doi.org/10.5194/acp-8-3093-2008

Turpin, B.J., Huntzicker, J.J. (1995). Identification of secondary organic aerosol episodes and quantification of primary and secondary organic aerosol concentrations during SCAQS. Atmos. Environ. 23, 3527–3544. https://doi.org/10.1016/1352-2310(94)00276-Q

U.S. EPA (2005). Guidelines for Carcinogen Risk Assessment, Risk Assessment Forum, Washington, D.C. EPA/630/P-03/001F.

U.S. EPA (2008). Integrated Risk Information System, Glossary of Terms. Office of Research and Development. Searched September 2008.

U.S. EPA (2009). Risk Assessment Guidance for Superfund Volume I: Human Health Evaluation Manual. Part F, Supplemental Guidance for Inhalation Risk Assessment. Washington, D.C., Office of Superfund Remediation and Technology Innovation, Environmental Protection Agency.

U.S. EPA (2011). Exposure Factors Handbook. 2011 edition. U.S. Environmental Protection Agency, Washington D.C.

Van Essen, H., Nieuwenhuijse, I., de Bruyn, S., Hoen, A. (2018). Health impacts and costs of diesel emissions in the EU. CE Delft. Report to the European Public Health Alliance (EPHA). Publication code: 18.4R30.140. 72 pp. https://cedelft.eu/wp-content/uploads/sites/2/2021/03/CE_Delft_4R30_Health_impacts_costs_diesel_emissions_EU_Def.pdf

Vega, E., Ruiz, H., Martinez-Villa, G., Sosa, G., Gonzalez-Avalos, E., Reyes, E., Garcia, J. (2007). Fine and coarse particulate matter characterization in a heavily industrialized city in central Mexico during Winter 2003. J. Air Waste Manage. Assoc. 57, 620–633. https://doi.org/10.3155/1047-3289.57.5.620

Vega, E., Escalona, S. (2009). Análisis químico de $PM_{2.5}$ y PM_{10} en la atmosfera de Cadereyta y ZMM. Proyecto F.21573. Informe Técnico Final. Instituto Mexicano del Petróleo.

Vega, E., Ruiz, H., Escalona, S., Cervantes, A., López-Veneroni, D., González Ávalos, E., Sánchez-Reyna, G. (2011). Chemical composition of fine particles in Mexico City during 2003-2004. Atmos. Pollut. Res. 2, 477–483. https://doi.org/10.5094/APR.2011.054

Viidanoja, J., Sillanpaa, M., Laakia, J., Kerminen, V.M., Hillamo, R., Aarnio, P., Koskentalo, T. (2002). Organic and black carbon in $PM_{2.5}$ and PM_{10}: 1 year of data from an urban site in Helsinki, Finland. Atmos. Environ. 36, 3183–3193. https://doi.org/10.1016/S1352-2310(02)00205-4

Wang, S., Ji, Y., Zhao, J., Lin, Y., Lin, Z., (2020). Source apportionment and toxicity assessment of $PM_{2.5}$-bound PAHs in a typical iron-steel industry city in northeast China by PMF-ILCR. Sci. Total Environ. 713, 136428. https://doi.org/10.1016/j.scitotenv.2019.136428

Wang, X., He, Sh., Chen, Sh., Zhang, Y., Wang, A., Luo, J., Ye, X., Mo, Z., Wu, L., Xu, P., Cai, G., Chen, Z., Lou, X. (2018). Spatiotemporal characteristics and health risk assessment of heavy metals in $PM_{2.5}$ in Zhejiang province. Int. J. Environ. Res. Public Health 15, 583. https://doi.org/10.3390/ijerph15040583

Watson, J.G., Chow, J.C., Engling, G., Chen, L.W.A., Wang, X.L. (2016). Source Apportionment: Principles and Methods. in: Harrison, R.M. (Ed.), Airborne Particulate Matter: Sources, Atmospheric Processes and Health. Royal Society of Chemistry, London, UK, pp. 72–125.

World Health Organization (WHO) (2000). Air Quality Guidelines for Europe, Part II Evaluation of Risks to Human Health, Chapter 5. Organic Pollutants European Series No. 91.

Xu, J., Jia, C., Yu, H., Xu, H., Ji, D., Wang, C., Xiao, H., He, J. (2021). Characteristics, sources, and health risks of $PM_{2.5}$-bound trace elements in representative areas of Northern Zhejiang Province, China. Chemosphere 272, 129632. https://doi.org/10.1016/j.chemosphere.2021.12

9632

Yang, L., Zhang, X., Xing, W., Zhou, Q., Zhang, L., Wu, Q., Zhou, Z., Chen, R., Toriba, A., Hayakawa, K., Tang, N. (2021). Yearly variation in characteristics and health risk of polycyclic aromatic hydrocarbons and nitro-PAHs in urban shanghai from 2010–2018. J. Environ. Sci. 99, 72–79. https://doi.org/10.1016/j.jes.2020.06.017

Yang, Y. Guo, P., Zhang, Q., Li, D., Zhao, L., Mu, D. (2010). Seasonal variation, sources and gas/particle partitioning of polycyclic aromatic hydrocarbons in Guangzhou, China. Sci. Total Environ. 408, 2492–2500. https://doi.org/10.1016/j.scitotenv.2010.02.043

Zambrano García, A., Medina Coyotzin, C., Rojas Amaro, A., López Veneroni, D., Chang Martínez, L., Sosa Iglesias, G. (2009). Distribution and sources of bioaccumulative air pollutants at Mezquital Valley, Mexico, as reflected by the atmospheric plant *Tillandsia recurvata* L. Atmos. Chem. Phys. 9, 6479–6494, https://doi.org/10.5194/acp-9-6479-2009

Zhang, J. Li, R., Zhang, X., Bai, Y., Cao, P., Hua, P. (2019). Vehicular contribution of PAHs in size dependent road dust: A source apportionment by PCA-MLR, PMF, and Unmix receptor models. Sci. Total Environ. 649, 1314–1322. https://doi.org/10.1016/j.scitotenv.2018.08.410

Zhang, Y., Tao, S. (2009). Global atmospheric emission inventory of polycyclic aromatic hydrocarbons (PAHs) for 2004. Atmos. Environ. 43, 812–819. https://doi.org/10.1016/j.atmosenv.2008.10.050

Zivin, J., Neidell, M. (2012). The impact of pollution on worker productivity. Am. Econ. Rev. 102, 3652–3673. http://doi.org/10.1257/aer.102.7.3652